Palaeogeography, Palaeoclimatology, Palaeoecology 403 (2014) 66–79

Contents lists available at ScienceDirect

Palaeogeography, Palaeoclimatology, Palaeoecology

journal homepage: www.elsevier.com/locate/palaeo

A diatom-based sea-ice reconstruction for the Vaigat Strait (Disko Bugt, West Greenland) over the last 5000 yr

Longbin Sha [a,b,*], Hui Jiang [c], Marit-Solveig Seidenkrantz [b], Karen Luise Knudsen [b], Jesper Olsen [d], Antoon Kuijpers [e], Yanguang Liu [f]

[a] Key Laboratory of Geographic Information Science, East China Normal University, 200062 Shanghai, PR China
[b] Centre for Past Climate Studies and Arctic Research Centre, Department of Geoscience, Aarhus University, DK-8000 Aarhus C, Denmark
[c] State Key Laboratory of Estuarine and Coastal Research and Key Laboratory of Geographic Information Science, East China Normal University, 200062 Shanghai, PR China
[d] Department of Physics and Astronomy, Aarhus University, DK-8000 Aarhus C, Denmark
[e] Geological Survey of Denmark and Greenland (GEUS), 1350 Copenhagen, Denmark
[f] Key Laboratory of Marine Sedimentology and Environmental Geology, First Institute of Oceanography, SOA, 266061 Qingdao, PR China

ARTICLE INFO

Article history:
Received 23 June 2013
Received in revised form 17 March 2014
Accepted 19 March 2014
Available online 27 March 2014

Keywords:
Diatoms
Sea-ice concentration (SIC)
Transfer function
West Greenland
Holocene

ABSTRACT

A diatom-based sea-ice concentration (SIC) transfer function was developed by using 72 surface samples from west of Greenland and around Iceland, and validated against associated modern SIC. Canonical correspondence analysis on surface sediment diatoms and monthly average of SIC indicated that April SIC is the most important environmental factor controlling the distribution of diatoms in the area, justifying the development of a diatom-based SIC transfer function. The agreement between reconstructed SIC based on diatoms from West Greenland and the satellite and modelled sea-ice data during the last ~75 yr suggests that the diatom-based SIC reconstruction is reliable for studying the palaeoceanography off West Greenland.

Relatively warm conditions with a strong influence of the Irminger Current (IC) were indicated for the early part of the record (~5000–3860 cal. yr BP), corresponding in time to the latest part of the Holocene Thermal Maximum. Between 3860 and 1510 cal. yr BP, April SIC oscillated around the mean value (55%) and during the time interval 1510–1120 cal. yr BP and after 650 cal. yr BP was above the mean, indicating more extensive sea-ice cover in Disko Bugt.

Agreement between reconstructed April SIC and changes in the diatom species suggests that the sea-ice condition in Disko Bugt was strongly influenced by variations in the relative strength of two components of the West Greenland Current, i.e. the cold East Greenland Current and the relatively warm IC. Further analysis of the reconstructed SIC record suggests that solar radiation may be an important forcing mechanism behind the historic sea-ice changes.

1. Introduction

Sea ice is a major component of the climate system, influencing the earth's albedo, as well as the exchanges of heat, moisture and gases between the ocean and the atmosphere. It is also a key environmental variable when assessing the magnitude and impact of future climate change because of its significant feedback on the planetary energy balance, deep ocean convection and marine biota (Miller et al., 2001), and it is one of the critical parameters in atmospheric and ocean models (Vinnikov et al., 1999). However, observed, reliable data such as satellite images, are only available for the last 30 yr with the exception of records from ship logs (Vinje, 2001), which are sporadic and irregular.

By extending sea-ice time series further back in time, the reconstruction of past sea-ice conditions may help palaeoclimate modellers to constrain boundary conditions and to validate model simulations (de Vernal and Hillaire-Marcel, 2000). Microfossils such as diatoms and dinoflagellate cysts are commonly used as proxies for reconstructing past sea-ice conditions, and a number of such studies have been carried out in the north-western North Atlantic region (De Sève and Dunbar, 1990; Koç Karpuz et al., 1993; Cremer, 1999; de Vernal and Hillaire-Marcel, 2000; Sarnthein et al., 2003; Müller et al., 2011; Weckström et al. 2013). However, only a few studies have focused on quantitative reconstructions of sea-ice concentration (SIC) (e.g. de Vernal et al., 2005), with a limited number of them determined using diatoms (Justwan and Koç Karpuz, 2008).

Diatoms are found widely in marine environments and are highly sensitive to ambient ecological conditions. The siliceous cell wall of diatoms is generally well-preserved in marine sediments, and changes in abundance and in species composition in the sediments can be used

* Corresponding author at: Key Laboratory of Geographic Information Science, East China Normal University, 200062 Shanghai, PR China. Tel.: +86 21 62233274; fax: +86 21 62232416.
E-mail address: shalongbin@hotmail.com (L. Sha).

http://dx.doi.org/10.1016/j.palaeo.2014.03.028
0031-0182/

for palaeoenvironmental interpretations. Whereas diatom-based transfer functions for sea ice have been widely developed in the Southern Ocean (Crosta et al., 1998, 2004; Gersonde et al., 2005), the North Pacific (Katsuki and Takahashi, 2005) and the northern North Atlantic (Justwan and Koç Karpuz, 2008), there has been a limited amount of marine diatom research in the north-western North Atlantic region.

The present paper studies the relationship between surface sediment diatoms and SIC in the north-western North Atlantic region and establishes a diatom-based SIC transfer function for this area. In this paper, we present a quantitative SIC record based on high-resolution diatom data for the NW Atlantic, and apply this transfer function to two marine sediment records in order to reconstruct palaeoclimatic and palaeoenvironmental changes off West Greenland during the mid- to late Holocene.

2. Study area

The investigated area extends from 50–75°N and covers the area between West Greenland and the Canadian Arctic Archipelago, which includes the Labrador Sea, Davis Strait and Baffin Bay (Fig. 1A). The Labrador Sea is connected with Baffin Bay through the Davis Strait gateway and with Hudson Bay through the Hudson Strait. A typical feature for West Greenland waters is low sea-surface temperatures all year round and summer air temperatures below 10 °C (Hansen et al., 2004). In the Labrador Sea, surface water temperatures vary between −1 °C in winter and 5–6 °C in summer while in Baffin Bay they are below −1 °C in winter, and vary from 4–5 °C in the southeast to 0 °C and below in the northwest during summer (Tang et al., 2004).

Disko Bugt is a large marine embayment (68°30′–69°15′N, 50°–54°W) in central West Greenland (Fig. 1B), ca. 150 km long and 100 km wide. Water depths generally range from 200 to 400 m, but reach up to 990 m in the deep submarine valley, Egedesminde Dyb, which extends in a south-western direction (Long and Roberts, 2003).

The Vaigat Strait is situated to the north (Fig. 1B) and is bounded by Disko Island to the southwest and the Greenland mainland to the northeast, and acts as a major exit route for the West Greenland Current (WGC) waters entering Disko Bugt, as well as for meltwater and icebergs produced by the major tidewater glaciers, including the Jacobshavn Isbræ, towards the north into Baffin Bay (Long and Roberts, 2003; Andresen et al., 2011). The strait is ca. 130 km long and 20–25 km wide and has maximum water depths of 600 m (cf. Andresen et al., 2011), and is believed that the passage acted as a northern conduit of an ice lobe extending to the mouth of the strait during the last glaciation (Weidick and Bennike, 2007).

The surface circulation west of Greenland and adjacent areas is dominated by two major currents: the WGC, which flows northward along the west coast of Greenland, and the Baffin–Labrador Current (BLC) that flows southward along the east coast of Baffin Island and Labrador (Fig. 1A). The WGC consists of two components, i.e. the cold low-salinity Polar water from the East Greenland Current (EGC) and the relatively warmer high-salinity Atlantic water from the Irminger Current (IC) (Andersen, 1981a; Buch, 2002; Tang et al., 2004). The two components mix continuously as it flows northwards, but can still be distinguished to the southwest of Disko Bugt (Andersen, 1981b). In western Baffin Bay, Arctic water is driven southward through the Canadian Archipelago, into Baffin Bay and Labrador Sea, and becomes the BLC (Drinkwater, 1996; Stern and Heide-Jørgensen, 2003; Tang et al., 2004).

Present-day observations indicate that in the Labrador Sea sea ice starts to form in November, with the maximum ice extent reached in March (LeDrew et al., 1992). The area off the Southwest Greenland coast, south of Nuuk, is normally free of sea ice, but during late winter or spring, as well as during early summer months it can be ice-covered for short periods by multi-year ice originating from the Arctic Ocean that drifts into the area (Valeur et al., 1997).

In Baffin Bay, sea ice starts to form in open waters in September, and cover increases steadily from the north to the south, reaching a maximum in March, when the entire bay, except for the eastern Davis Strait,

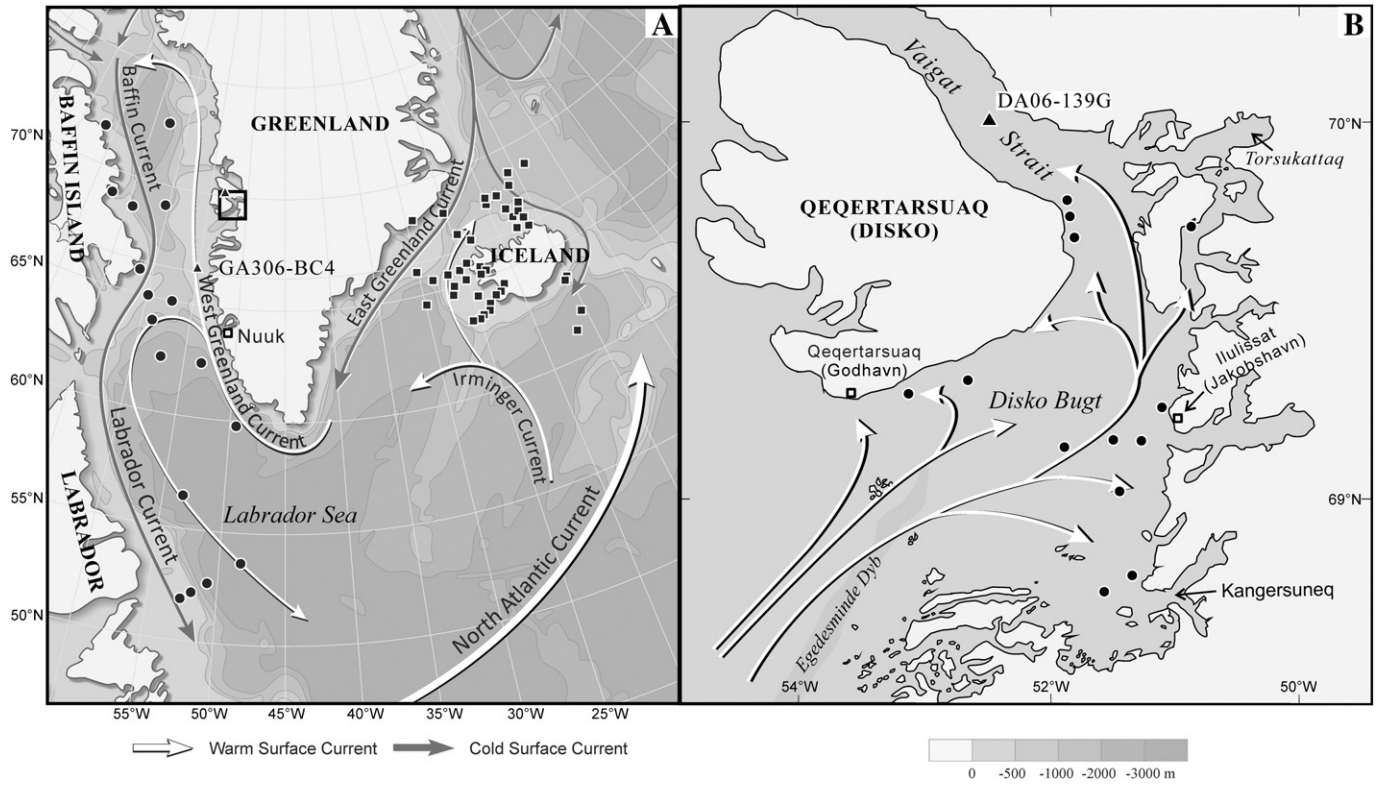

Fig. 1. (A) Surface current pattern in the NW Atlantic and locations of diatom samples in the investigated area. (B) Detailed map of the study area shown as a square on Fig. 1A. Filled circles indicate new samples from off West Greenland. Filled squares represent samples from off East Greenland and Iceland previously published by Jiang et al. (2001).

is covered by ice (Tang et al., 2004). In winter, the bay is also covered by seasonal land-fast sea ice with a mean thickness of ca. 0.7 m (Buch, 2000). During the 1990s, the duration of sea-ice cover in Disko Bugt has decreased from 5 months in the beginning of the interval to about 3 months in later years because of milder winter temperatures (Nielsen et al., 2001).

The majority of icebergs in Baffin Bay are produced by the glaciers north of 68°N on the west coast of Greenland, with the most productive in Disko Bugt and Umanak Bay (Tang et al., 2004). Many of the icebergs produced in Disko Bugt leave Baffin Bay and enter into the Labrador Sea through the Davis Strait.

3. Materials and methods

3.1. Palaeo-records: sediment cores and diatom samples

A 446 cm long gravity core, DA06-139G (Fig. 1B), was collected from Vaigat Strait in Disko Bugt at 70°05.486′N, 52°53.585′W (water depth 384 m) during a cruise on the Danish research vessel 'Dana' in 2006 (Dalhoff and Kuijpers, 2007). For further description see Andresen et al. (2011). A total of 90 samples (a 1-cm sediment sample taken every 5 cm) from core DA06-139G was analysed for their diatom content throughout. A 35-cm long box core GA306-BC4 (Fig. 1A) from a submarine valley, Holsteinsborg Dyb, West Greenland (see Supplementary Information and Sha et al., 2012), was used to test the reliability of the diatom-inferred SIC reconstruction by comparing it with instrumental and documentary data for the area.

The samples from gravity core DA06-139G were prepared according to the method described by Håkansson (1984) and Sha et al. (2012). More than 300 diatom valves were counted in random transects for each sample (excluding *Chaetoceros* resting spores, cf. Koç Karpuz and Schrader, 1990; Cremer, 1999). Diatom percentages were calculated based on the diatom sum, excluding *Chaetoceros* resting spores.

3.2. Age model of sediment cores

The chronology of gravity core DA06-139G was constrained by 10 AMS ^{14}C dates on molluscs, marine plant (sea grass) fragments and one sample of mixed benthic foraminifera (Table 1). All ^{14}C ages are calibrated with the OxCal 4.1 software (Ramsey, 2008) using the Marine09 calibration data set (Reimer et al., 2009) with a local marine reservoir age ΔR of 140 ± 30 (McNeely et al., 2006; Lloyd et al., 2011). An age model was constructed by using the depositional model option in OxCal with a k value of 100, yielding A_{model} = 52.0% (Fig. 2). Note that the age model used in this study has changed slightly compared to that presented by Andresen et al. (2011). The age model of box core GA306-BC4 is presented in Sha et al. (2012; see also Supplementary Information).

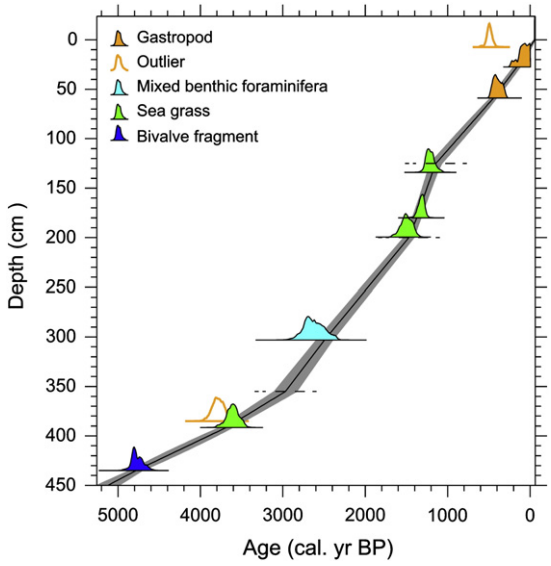

Fig. 2. Age-depth model for gravity core DA06-139G in Vaigat Strait, Disko Bugt, West Greenland. Note that the age model has changed slightly compared to that presented by Andresen et al. (2011).

3.3. Modern diatom data

The surface diatom samples from West Greenland were collected from the uppermost 1 cm of sediment by using a Van Veen sampler during a cruise on the Danish research vessel 'Porsild' in 1999 (Lloyd, 2006b), as well as from box cores obtained from the German research vessel 'Maria S. Merian' in 2008. The sampling methods are listed in Supplementary Table 1. These surface samples were prepared following the methods described above. Diatom data from areas that are strongly influenced by the EGC and IC waters, e.g. around Iceland, were also included in the modern data set since the WGC is composed of the both EGC and IC waters (cf. Jiang et al., 2001). In total, surface sediment diatom data from 72 surface samples were used in the modern calibration data set.

3.4. Modern SIC data

The modern sea-ice distribution data used in this study were collected from Nimbus-7 SMMR and DMSP SSM/I-SSMIS Passive Microwave Data (GSFC product, NSIDC-0051). The data are provided in the polar stereographic projection at a grid cell size of 25 × 25 km, and include gridded daily (every other day for SMMR data) and monthly averaged SIC for both the north and south polar regions since 26 October 1978 (Cavalieri et al., 1996). A monthly mean of the SIC percentage (percent area per unit area) since 1979 is available for each surface sediment

Table 1
AMS ^{14}C age determinations from core DA06-139G.

Laboratory no.	Material	Core depth (cm)	δ^{13}C (‰ VPDB)	^{14}C age (BP ± 1σ)	ΔR (yr)	Reservoir corrected ^{14}C age (BP ± 1σ)	Model age (cal. yr BP)
AAR 10953	Gastropod	7–8	0.07	1013 ± 35	140 ± 30	873 ± 46	34 ± 33
AAR13060	Gastropod	27–28	−0.05	607 ± 22	140 ± 30	467 ± 37	185 ± 38
AAR 10952	Gastropod	58–60	0.26	903 ± 35	140 ± 30	763 ± 46	453 ± 33
AAR 10951	Plant fragment (sea grass)	132–136	−16.52	1797 ± 40	140 ± 30	1657 ± 50	1189 ± 62
AAR13059	Plant fragment (sea grass)	180	−17.03	1913 ± 27	140 ± 30	1773 ± 40	1383 ± 52
AAR 10950	Plant fragment (sea grass)	199–200	−16.87	2090 ± 42	140 ± 30	1950 ± 52	1479 ± 63
AAR 13061	Mixed benthic foraminifera	302–304	*0	3030 ± 90	140 ± 30	2890 ± 95	2502 ± 99
AAR 10949	Gastropod	385	−0.4	3976 ± 38	140 ± 30	3836 ± 48	3568 ± 89
AAR 10948	Plant fragment (sea grass)	390–393	−16.89	3833 ± 43	140 ± 30	3693 ± 52	3696 ± 75
AAR 10947	Bivalve shell	435	1.94	4709 ± 40	140 ± 30	4569 ± 50	4793 ± 73

*δ^{13}C estimated.

sample site and used as the environmental variables in this study (Supplementary Table 2).

4. Results

4.1. Modern diatom-SIC data set

Canonical correspondence analysis (CCA) was employed to identify statistically significant relationships between the diatom assemblages and the environmental variables (See Supplementary Information). The eigenvalues of CCA axes 1 and 2 are 0.441 and 0.165, respectively, indicating that axis 1 captures most of the variance in the data set and therefore is most important. The species-environment correlations for CCA axes 1 and 2 are high (0.947, 0.857). The computer intensive method of Unrestricted Monte Carlo permutation tests (999 permutations under the null model) on the first ordination axis and the canonical axes together based on their *p*-values demonstrate that both are statistically significant ($p = 0.001$).

To avoid using strongly correlated variables in CCA, variables with a variance inflation factor (VIF) >20 (January, February, March, May, June, July, September and December SICs) were removed from the analysis (cf. ter Braak, 1986). For the remaining four variables, forward selection of the environmental variables and associated Monte Carlo permutation test (999 permutations) was used to examine whether an individual variable was statistically significant. The result reveals that only April and August SICs explained a statistically significant ($p \leq 0.001$) amount of variation in the diatom data.

Forward selection with Monte Carlo significance tests showed that April SIC along captures 38% of the canonical variance, suggesting that April SIC is the most important environmental factor controlling the distribution of diatoms in the surface sediments. This also makes ecological sense since April is one of the months for diatom blooms, when the light and temperature are often optimal, and melting ice produces water of significantly lowered salinity (Krebs, 1983; Williams, 1986). Consequently, April SIC may potentially be reconstructed by using diatoms preserved in the sediments.

4.1.1. Surface sample species distribution

In the CCA plot, the diatom species are positioned based on their relationship to the environmental variables used in the ordination (Fig. 3). The species predominantly influenced by the SIC generally plot to the right of CCA axis 2 (with high positive values on the SIC 'axes'), e.g. *Fragilariopsis cylindrus*, *Fossula arctica*, *Detonula confervaceae* resting spores and *Thalassiosira bulbosa* (Fig. 3). Based on the modern samples, these species were most abundant in Baffin Bay, the western Davis Strait, Disko Bugt and the East Greenland coast, the areas which are covered with sea ice and icebergs for a longer period of time each year. The species in this group are thus associated with higher SIC.

In contrast to the sea-ice species above, taxa plotting to the left of CCA axis 2 are *Thalassionema nitzschioides*, *Thalassiosira oestrupii*, *Rhizosolenia hebetata* f. *semispina*, *Neodenticula seminae* and *Rhizosolenia borealis*. They have the highest abundances at the sites south and west of Iceland, as well as south of the Labrador Sea, which are normally free of sea ice. These species are here associated with the low SIC.

Species that are common in most of the samples analysed plot towards the middle of the ordination diagram and have medium values on the SIC 'axes'. They include species such as *Thalassiosira nordenskioeldii*, *Thalassiosira antarctica* var. *borealis* resting spores, *Fragillariopsis oceanica*, *Bacterosira bathyomphala*, *Thalassiosira antarctica* vegetative cells and *Thalassiosira hyalina*.

4.1.2. Sample sites and their correlation with environmental variables

The positions of the samples in the CCA ordination diagram and their relationship to the two environmental variables are shown in Fig. 4. Overall, CCA axis 2 separates sample sites linked to the high SIC (right of the CCA axis 2) in areas which today are strongly influenced by Polar waters (e.g. those in Baffin Bay, Disko Bugt and the East Greenland coast) from those in areas influenced by Atlantic water and the low SIC (left of the CCA axis 2; west and south of Iceland, and the southernmost Labrador Sea).

Most of the sample sites from Baffin Bay and the coast of East Greenland have high positive values on the April SIC 'axis' but only medium values on the August SIC 'axis', suggesting that they reflect high April SIC but relatively moderate August SIC, as also shown in present day observations with the most extensive sea-ice cover in spring (Tang et al., 2004). Almost all samples from the Disko Bugt plot in the same environmental space associated with the April SIC axis, implying that they are characterized by high April SIC and different August SIC. The sample sites from the northern Labrador Sea have medium values on the April and August SIC 'axes', suggesting that they are indicative of a cold, ice-free to seasonally ice-covered waters. The sample sites around Iceland, as well as the southernmost Labrador Sea, plot to

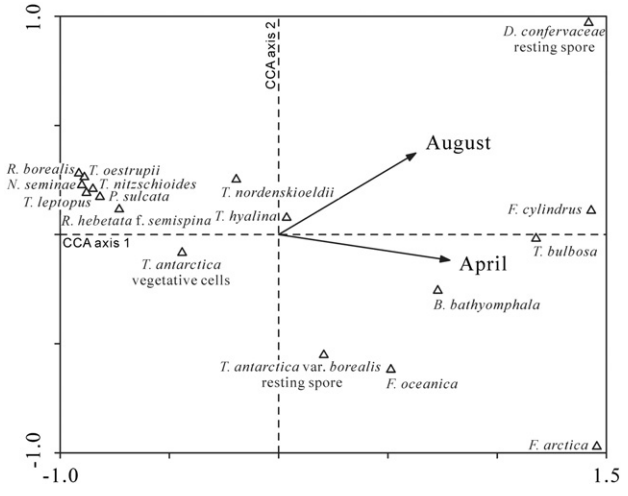

Fig. 3. Canonical correspondence analysis (CCA) biplot of surface sample diatom species and environmental variables with grouping of diatom species.

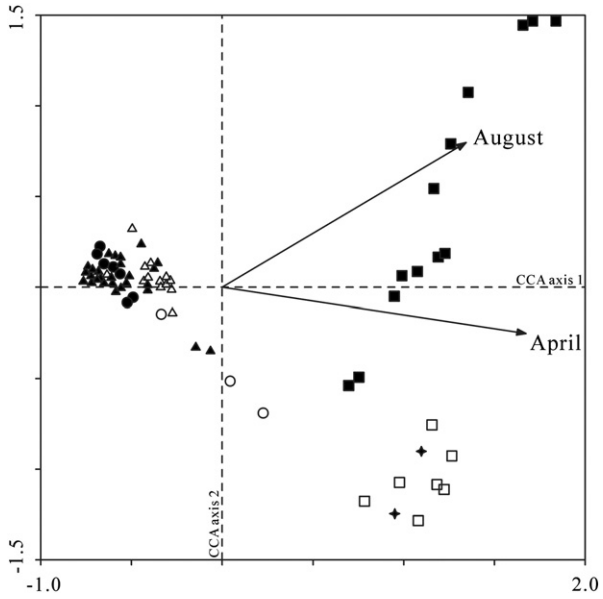

Fig. 4. Canonical correspondence analysis (CCA) biplot of diatom surface samples and environmental variables focusing on the surface samples. The symbols for samples are: empty square (Baffin Bay), filled square (Disko Bugt), filled asterisk (East Greenland coast), empty triangle (north of Iceland), empty circle (northern Labrador Sea), filled circle (southern Labrador Sea) and filled triangle (west and south of Iceland).

Table 2
Results of method testing for the transfer function. Maximum bias (Max $Bias_{(Jack)}$), coefficient of determination between observed and predicted values R^2_{Jack}, and root-mean squared error of prediction, based on the leave-one-out jack-knifing ($RMSEP_{(Jack)}$) for the reconstructed April SIC in seven reconstruction procedures. WA = weighted averaging regression and calibration, $WA_{(tol)}$ = weighted averaging with tolerance down-weighting, PLS = partial least squares, WA-PLS = weighted averaging with partial least squares and MAT = Modern analogue technique. Both inverse and classical deshrinking regression were used in WA and $WA_{(tol)}$ reconstruction procedures. The tests show that WA-PLS with 3 components is the most reliable (values in bold).

		Max $Bias_{(Jack)}$	R^2_{Jack}	$RMSEP_{(Jack)}$
WA	Inverse	1.06306	0.837214	1.4806
$WA_{(tol)}$	Inverse	2.95589	0.81812	1.58468
WA	Classical	0.651756	0.838939	1.56304
$WA_{(tol)}$	Classical	2.93477	0.819548	1.71577
PLS	1 component	1.58981	0.798683	1.64734
PLS	2 component	2.09924	0.891266	1.20995
PLS	3 component	2.30016	0.901447	1.15209
PLS	4 component	2.03214	0.906372	1.1239
PLS	5 component	1.96989	0.906933	1.1223
WA-PLS	1 component	1.11848	0.837833	1.47897
WA-PLS	2 component	2.37824	0.915339	1.07121
WA-PLS	3 component	**1.81278**	**0.916279**	**1.06488**
WA-PLS	4 component	1.8085	0.905789	1.13729
WA-PLS	5 component	2.17254	0.894113	1.21179
MAT	1 analogues	2.83904	0.850474	1.4588
MAT	2 analogues	3.32066	0.876052	1.30939
MAT	3 analogues	3.19086	0.910639	1.1037
MAT	4 analogues	3.45697	0.909175	1.11335
MAT	5 analogues	2.21228	0.903406	1.15098

the left of CCA axis 2, showing that they are characterized by low SIC and ice-free waters.

4.2. Diatom-based transfer function for palaeo-April SIC

To establish a transfer function with the least error, several parameters, presented as root-mean squared error of prediction, based on the leave-one-out jack-knifing ($RMSEP_{(Jack)}$) test, maximum bias in jack-knife residuals, and coefficient of determination between observed and predicted values R^2_{Jack}, are applied to evaluate seven numerical reconstruction methods (Table 2). A reliable transfer function should thus have a low $RMSEP_{(Jack)}$ and maximum bias, as well as a high R^2_{Jack} (Birks, 1995, 1998). The results show that weighted averaging with partial least squares regression (WA-PLS) using 3 components has the lowest $RMSEP_{(Jack)}$ (1.06488) and the highest R^2_{Jack} (0.916279) for April SIC (Table 2), and hence, the WA-PLS using 3 components should be employed to obtain the most reliable diatom-based SIC in the area.

The performance of the final model is illustrated in the plots of observed values against predicted and residual (predicted-observed) values (using cross-validated models), which display a linear relation between observed and predicted SICs from surface samples (Fig. 5).

A dinocyst-based sea-ice transfer function using the Modern Analog Technique has previously been developed and successfully applied to reconstruct past sea-ice over the northern North Atlantic during the last Glacial Maximum and the Holocene (de Vernal and Hillaire-Marcel, 2000, 2006; de Vernal et al., 2005, 2013a, 2013b, 2013c). Each sea-ice proxy has limitations and uncertainties due to its respective distribution and its preservation through time (de Vernal et al., 2013a). Seidenkrantz (2013) compared the diatom sea-ice data (Knudsen et al., 2008) with dinocyst sea-ice records (Levac et al., 2001) from the same core (HU91-039-008P), and found a correlation coefficient of 0.37, indicating that there is a link between the different sea-ice proxies, but also that they presumably describe different aspects of sea-ice cover. We here suggest that this difference is that while the dinocyst data seem to describe the duration of sea-ice cover, the diatoms are primarily linked to sea-ice cover in a certain part of the year.

4.3. Reliability of the diatom-based palaeo-April SIC reconstruction

In order to test the reliability of the diatom-based April SIC reconstruction as a measure for palaeoceanographic changes in Disko Bugt further back in time, the reconstructed April SIC for box core GA306-BC4 (Supplementary Information) was compared with satellite April SIC from Nimbus-7 SMMR and DMSP SSM/I-SSMIS Passive Microwave Data (GSFC product, NSIDC-0051) for the period AD 1979–2006 (Fig. 6). Additionally, the data were compared with modelled April SIC from the Hadley Centre sea-ice and sea-surface temperature (SST) data set version 1.1 (HasISST 1.1), provided by the Met Office Hadley Centre for Climate Prediction and Research (Rayner et al., 2003), for the time period AD 1953–2006, as well as with mean water temperature in the upper 200 m west of Fylla Bank (Section 4) for AD 1963–2006.

A general rise in the diatom-based SIC was observed between the mid-1950s and the mid-1970s, a feature which is also found in the modelled sea-ice records from the same area. At Fylla Bank (Section 4), there was a similar apparent reduction in the inflow of IC (Buch et al., 2004). From the mid-1970s to the late 1980s, there was an interval with decreased reconstructed SIC, followed by an increase towards the upper part of this period. A similar trend has been observed

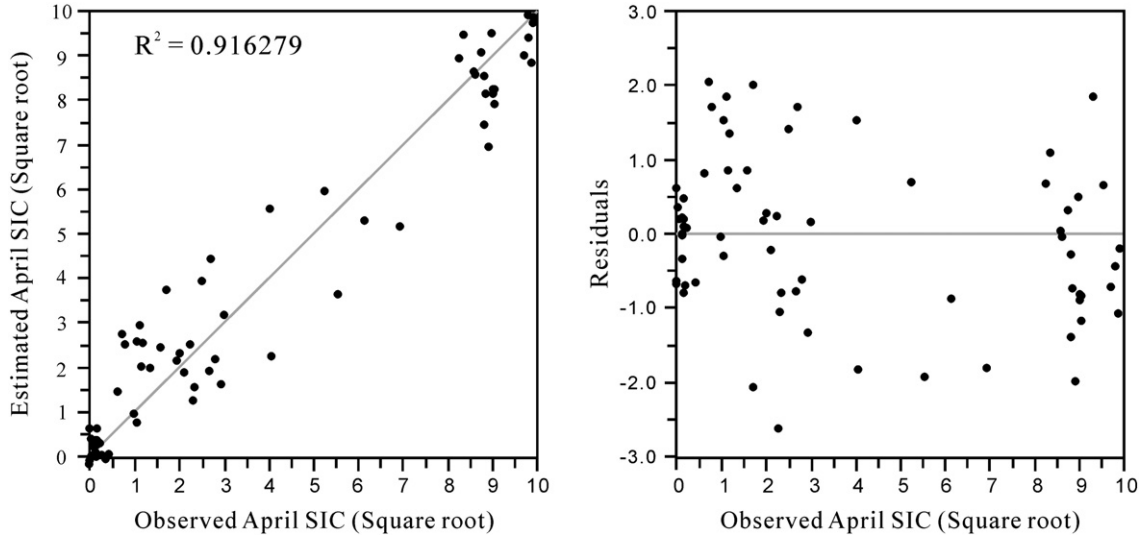

Fig. 5. Plots of observed versus predicted values and observed versus residual (predicted minus observed) values for the final transfer function model derived for April sea-ice concentrations. The SIC percentage was transformed to square-roots.

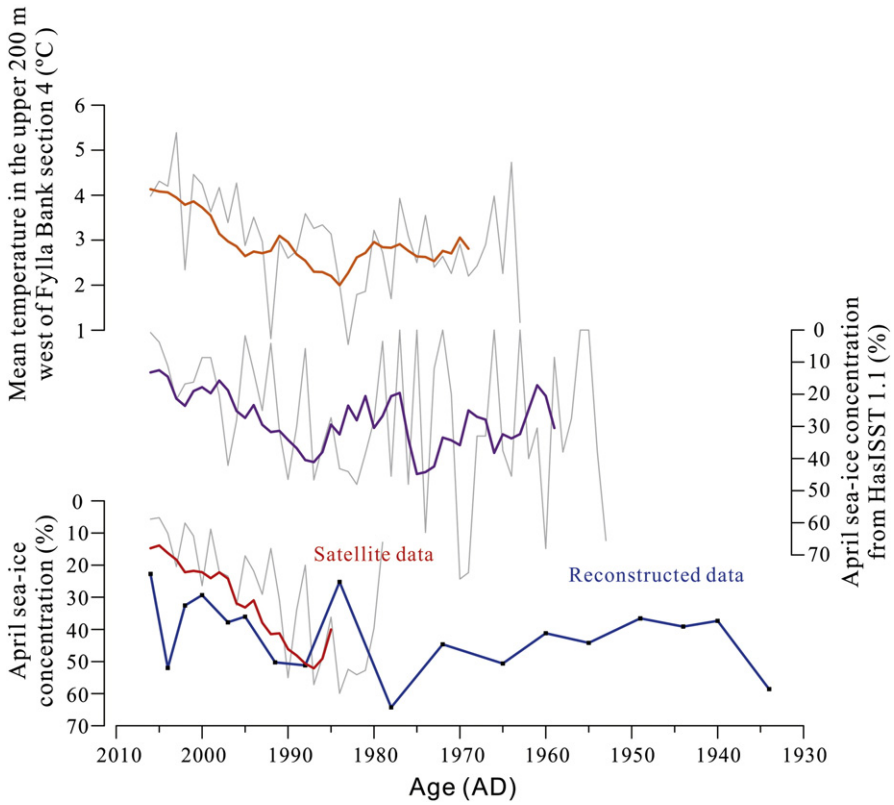

Fig. 6. Diatom-based reconstructed April sea-ice concentration (blue) for the period AD 1935–2006 compared with the satellite April sea-ice concentration (red) from Nimbus-7 SMMR and DMSP SSM/I-SSMIS Passive Microwave Data (GSFC product, NSIDC-0051) for the period AD 1979–2006 and the modelled April sea-ice concentration (purple) from the HasISST 1.1 data set (AD 1953–2006), as well as mean temperature in the upper 200 m (orange) west of Fylla Bank (Section 4) for AD 1963–2006. Actual data are shown as grey lines; smoothed records (7-point weighted moving average) are denoted by bold lines in colour.

in the modelled sea-ice data from HasISST 1.1 data set, although with a few temporal differences, which may be caused by uncertainties in the chronology and the low temporal resolution of the sediment core.

After AD 1990, there was a pronounced decline in reconstructed SIC, reaching the minimum value at the core surface. A similar warming trend, during the same period, was also observed in the satellite sea-ice data and modelled sea-ice records, as well as in the sea temperature of the upper 200 m indicating a reduction of the strength of the EGC after AD 1990 and/or a more dominant influence of IC. SIC increased around AD 2004, however, indicating an extensive sea-ice cover, as also reflected in observation records of winter Northern Hemisphere sea-ice extent (Walsh, 1978).

In summary, there is a reasonably high degree of similarity between the diatom-based reconstructed April SIC and the satellite and modelled sea-ice data, as well as with instrumental temperature records, although interestingly the correlation to satellite data is better than the correlation to the modelled data. This overall good correlation suggests that the diatom-based SIC transfer function may be used for studying palaeoceanography and palaeoclimate off West Greenland at pre-instrumental times.

4.4. Diatom stratigraphy and palaeoenvironments in core DA06-139G

As an illustration of the palaeoceanographic changes in Disko Bugt during the past 5000 yr, percentages of the most important diatom species with specific environmental significance from gravity core DA06-139G are presented in Fig. 7. The main taxa in this core are *T. antarctica* var. *borealis* resting spores, *F. cylindrus*, *F. oceanica*, *T. nordenskioeldii*, *D. confervaceae* resting spores, *T. antarctica* vegetative cells, *B. bathyomphala*, *T. bulbosa*, *T. hyalina*, *F. arctica* and *T. nitzschioides* (Fig. 7). The diatom record has been divided into six assemblage zones (Fig. 7) using cluster analysis (Grimm, 1987).

4.4.1. Zone I, 5000–3860 cal. yr BP, 443.5–398 cm

The diatom assemblage was dominated by *T. antarctica* var. *borealis* resting spores with the highest contribution up to more than 60%. *T. nitzschioides* reached relatively high numbers in this zone, although the values are low (1–2%). Abundances of *F. cylindrus* and *D. confervaceae* resting spores were also low, whereas *F. arctica* and *T. bulbosa* were rare or absent.

Today, resting spores of *T. antarctica* var. *borealis*, an Arctic neritic taxon, are found in northern cold-water to temperate regions (Hasle and Syvertsen, 1997; von Quillfeldt, 2000; Krawczyk et al., 2010), and it is the dominant taxon of the Arctic water surface sediment assemblages in the Nordic Seas (Koç Karpuz and Schrader, 1990). It is widely distributed in surface sediments from the Labrador Sea (De Sève, 1999) and dominated the sedimentary record in Disko Bugt (cf. Jensen, 2003).

T. nitzschioides is the main species in warmer Atlantic waters (e.g. Koç Karpuz and Schrader, 1990; Jiang et al., 2001), and its abundance decreases as the IC waters flow from the Irminger Sea and clockwise around Iceland and southern Greenland. The species has the greatest abundance south of Iceland and decreases towards the west and north of Iceland. In surface sediments in Disko Bugt, to the west of Greenland, the abundance of *T. nitzschioides* is only about 0–1%. Therefore, it can be used as a measure of the influence of warmer, Atlantic-derived water masses, although its absolute values are low (cf. Sha et al., 2012). The diatom assemblage in zone I suggests that

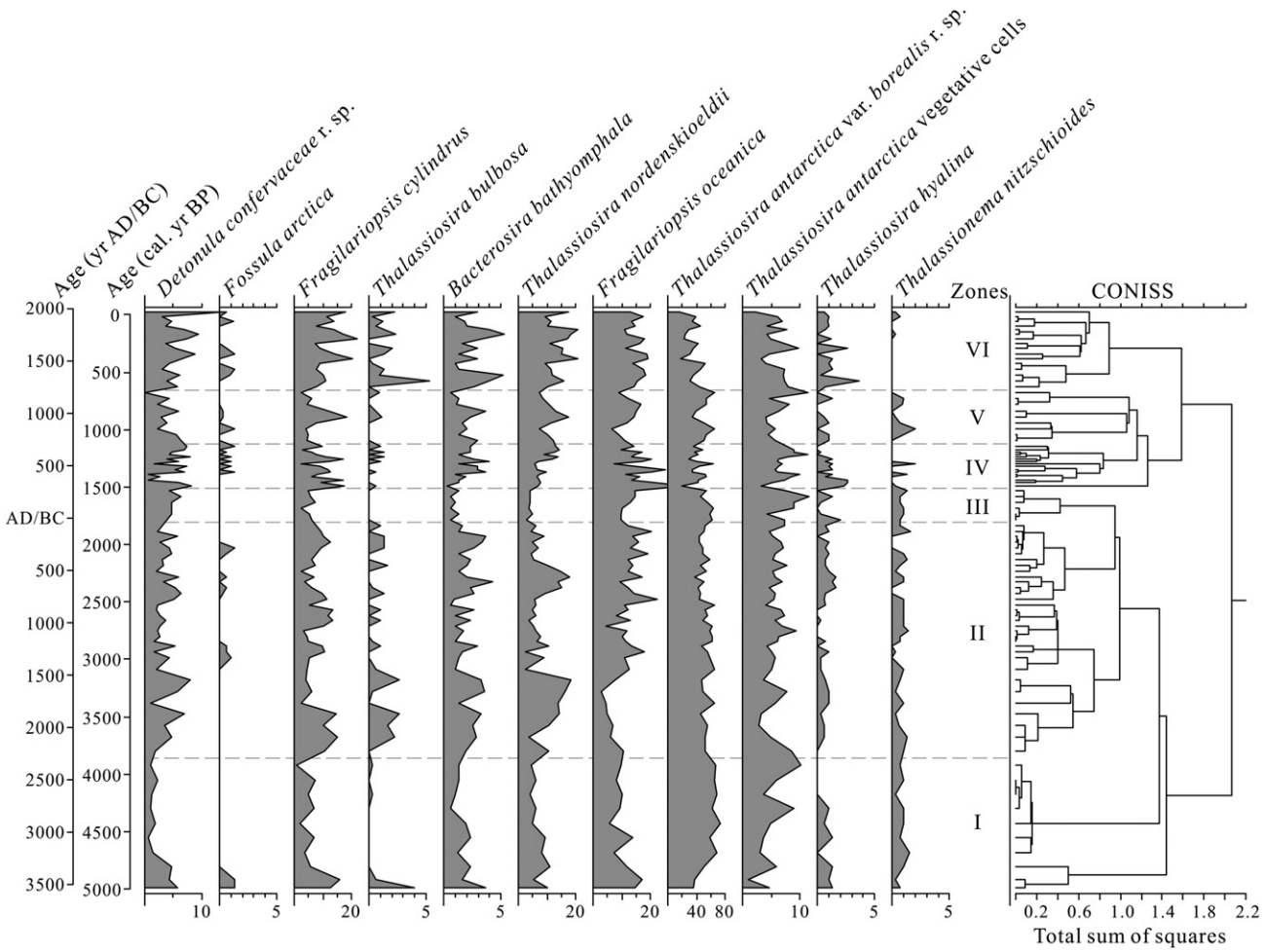

Fig. 7. Distribution (percentages, excluding *Chaetoceras* resting spores) of the most common diatoms in the studied record of core DA06-139G. The diatom zonation is based on cluster analysis. r. sp. = resting spores. The ages are shown on a 'cal. yr BP' scale, as well as a 'yr AD/BC' scale.

the Atlantic water influence was relatively strong with less SIC than at present.

4.4.2. Zone II, 3860–1810 cal. yr BP, 398–233 cm

T. antarctica var. *borealis* resting spores were still the main component of the assemblage, but a rapid increase in abundance of *D. confervaceae* resting spores, *F. cylindrus*, *F. arctica* and *T. bulbosa*, as well as *B. bathyomphala* and *T. nordenskioeldii* characterizes the zone. The abundance of *T. nitzschioides* decreased slightly and was also absent during short intervals.

F. cylindrus is a bipolar planktonic species associated with sea ice (Medlin and Priddle, 1990; Hasle and Syvertsen, 1997). It is among the dominant species in the Barents Sea and off Northeast Greenland (von Quillfeldt, 2000), as well as in Disko Bugt, West Greenland (Jensen, 2003; Krawczyk et al., 2010). *D. confervaceae* is regarded as a sea-ice taxon in the Laptev Sea (Bauch and Polyakova, 2000; Polyakova, 2001). *T. bulbosa* has been found growing in sea ice or in the water close to the edge of sea ice, often being one of the dominant taxa (Syvertsen and Hasle, 1984). *F. arctica* is an Arctic, neritic species closely associated with sea ice (von Quillfeldt, 1996), and was observed in Holocene sedimentary records in Disko Bugt (Jensen, 2003; Krawczyk et al., 2010) and the Nares Strait (Knudsen et al., 2008). These four taxa were the main components of the sea-ice diatom assemblage off West Greenland, indicating high SIC (Fig. 3).

B. bathyomphala is found in the northern cold-water region (Hasle and Syvertsen, 1997) and was the main species of the Arctic diatom assemblage around Iceland, indicating the influence of Arctic water masses from the East Icelandic Current (Jiang et al., 2001). *T. nordenskioeldii*, a neritic species usually living in cold to temperate areas (Hasle and Syvertsen, 1997), is the dominant species in surface sediment assemblages off West Greenland. An increase in the abundances of sea-ice diatoms together with Arctic water species suggests more severe sea-ice condition in this time interval than for Zone I.

4.4.3. Zone III, 1810–1510 cal. yr BP, 233–203 cm

The main components of the zone were similar to those of Zone I, and it was characterized by an abrupt decline or even absence of the sea-ice species *F. cylindrus*, *F. arctica* and *T. bulbosa* and a continuous occurrence of the warm-water species *T. nitzschioides*. This assemblage indicates a short interval of enhanced Atlantic water influx and somewhat reduced SIC.

4.4.4. Zone IV, 1510–1120 cal. yr BP, 203–123 cm

An increased importance of the sea-ice species *F. cylindrus*, *F. arctica* and *T. bulbosa*, as well as in Arctic water species *B. bathyomphala* and *T. nordenskioeldii*, suggests a period of extended sea-ice cover. A marked decline or even disappearance of the warm-water species *T. nitzschioides* indicates a reduced influence of Atlantic waters in the region.

4.4.5. Zone V, 1120–650 cal. yr BP, 123–78 cm

After 1100 cal. yr BP, *T. nitzschioides* increased, reaching almost the same level as between 5000 and 3860 cal. yr BP, coinciding with reduced abundance of sea-ice species and Arctic species suggesting an increase in the influence of Atlantic water.

4.4.6. Zone VI, after 650 cal. yr BP, 78–0 cm

In Zone VI, species associated with sea ice (*F. cylindrus*, *D. confervaceae* resting spores, *T. bulbosa*, *F. arctica*, *B. bathyomphala* and *T. nordenskioeldii*) reached their highest abundances. Concurrently, the Atlantic water species *T. nitzschioides* almost completely disappeared. This assemblage suggests that the region experienced the most extensive sea-ice cover during this time period, and that there was only little influence of Atlantic water.

4.5. Reconstruction of April SIC for the last 5000 yr

The diatom-based SIC transfer function was applied to the diatom assemblages from core DA06-139G to establish an April SIC record for approximately 5000 cal. yr BP in the Disko Bugt area (Fig. 8). The reconstructed April SIC in Disko Bugt varied between 25 and 95% with a mean value around 55% over the last 5000 yr. It was generally below the mean value (55%) (less extensive) before 3860 cal. yr BP except for a short period around 4900 cal. yr BP, and was above the mean after 1510 cal. yr BP (Fig. 8). It oscillated around the mean between 3860 and 1510 cal. yr BP, with relatively high values around ca. 3700–3500, 3000–2800 and 2200–1900 cal. yr BP. The April SIC increased to approximately 20–30% above the mean during the period 1510–1120 cal. yr BP and dropped below the mean between 1120 and 650 cal. yr BP. After 650 cal. yr BP, there was an abrupt increase in the April SIC suggesting that increased sea-ice cover generally prevailed in the study area. A short-term SIC decrease after 60 cal. yr BP indicated the end of this high sea-ice cover period.

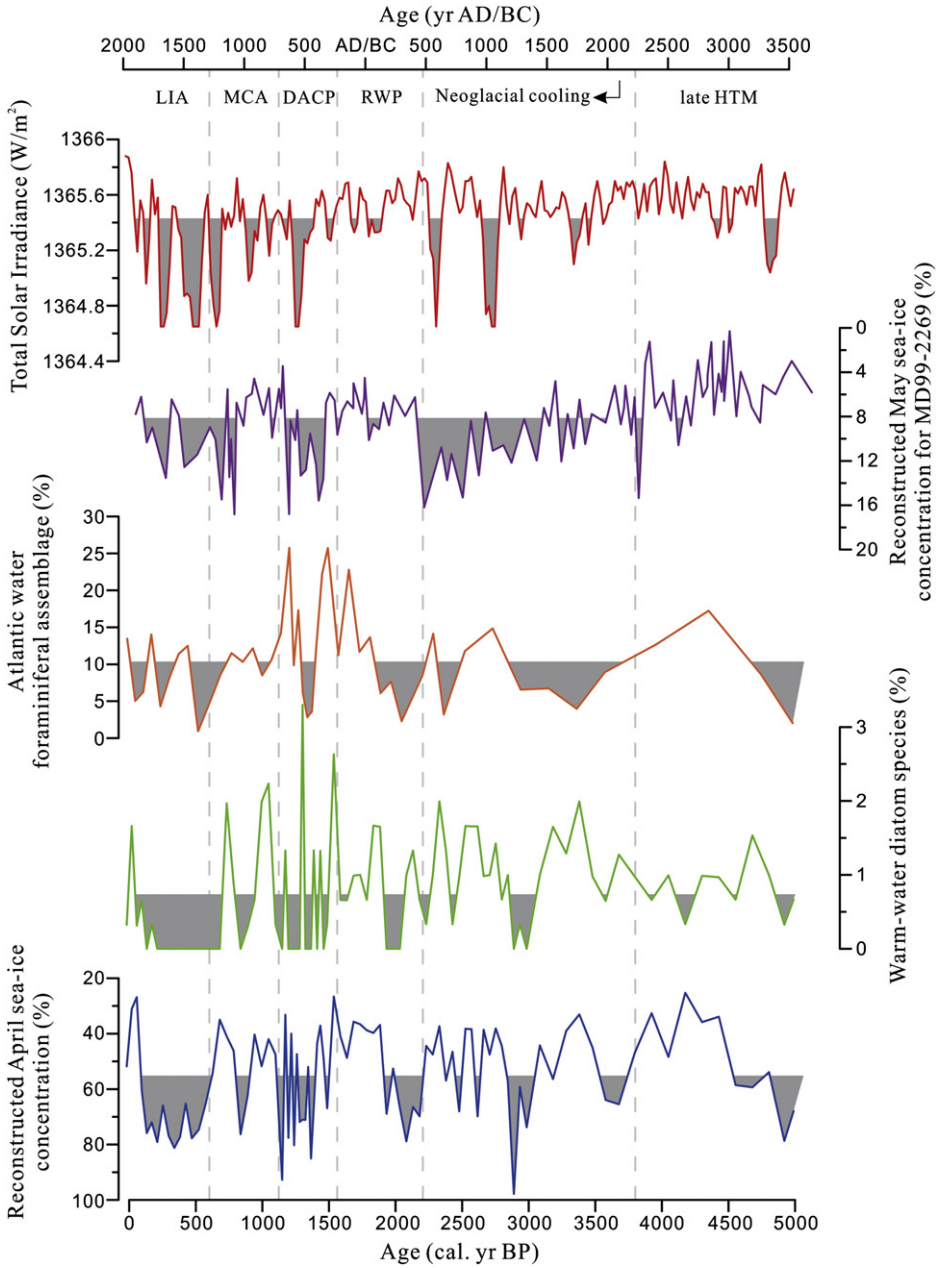

Fig. 8. The relationship between the reconstructed April sea-ice concentrations of marine sediment core DA06-139G, changes in warm-water diatom taxa and Atlantic foraminiferal assemblage, the reconstructed May sea-ice concentration based on diatom data from core MD99-2269 on the North Iceland shelf (Justwan and Koç Karpuz, 2008), as well as total solar irradiance variations constructed from the ^{10}Be record in the Greenland and Antarctica ice cores and tree-ring records of ^{14}C fluctuations (Steinhilber et al., 2012). The limit of grey shading indicates mean value for each record. Approximate time intervals for historical NE Atlantic climate events are shown (LIA = 'Little Ice Age'; MCA = 'Medieval Climate Anomaly'; DACP = 'Dark Ages Cold Period'; RWP = 'Roman Warm Period'; HTM = 'Holocene Thermal Maximum'). The ages are shown on a 'cal. yr BP' scale, as well as a 'yr AD/BC' scale.

5. Discussion

5.1. Latest part of the Holocene Thermal Maximum

The diatom-inferred SIC indicates reduced sea-ice cover and relatively warm conditions in Disko Bugt during the period 5000–3860 cal. yr BP (Fig. 8). This coincided with a period of few sea-ice species and relatively high abundances of warm-water diatom taxa (Figs. 7, 8), suggesting that a generally high influx of Atlantic waters to the region was the main factor driving the decline of SIC. There was a clear spatial difference in the timing of the Holocene Thermal Maximum (HTM) in the Northern Hemisphere and in the Greenland region (Dahl-Jensen et al., 1998; Kaplan et al., 2002; Kaufman et al., 2004). The period 5000–3860 cal. yr BP may be referred to as the final part of the HTM, as also previously suggested by Andresen et al. (2011) and McCarthy (2011) using the same core as in this study and by Erbs-Hansen et al. (2013) from a study located in the Holsteinsborg Dyb. High abundances of Atlantic water foraminifera also indicated a high influx of Atlantic waters during this period (Fig. 8; Andresen et al., 2011).

Møller et al. (2006), Seidenkrantz et al. (2007) and Ren et al. (2009) also recognized a relatively warm, final part of the HTM in a fjord just south of Nuuk in West Greenland, and they ascribed this to a persistent and relatively high influx of Atlantic-source water to the WGC. Relatively warm conditions in Disko Bugt, with low SIC, is in accordance with dinocyst assemblage data from northernmost Baffin Bay, which exhibited higher than present sea-surface temperatures and a short sea-ice season between ca. 6800 and 3500 cal. yr BP (Levac et al., 2001). Foraminiferal data from the same site also suggest a relatively strong northward flow of WGC waters (Knudsen et al., 2008).

Additionally, a 7000-yr long spring sea-ice record in the Canadian Arctic Archipelago, determined by quantification of the sea-ice biomarker IP_{25}, showed IP_{25} fluxes consistently below the mean values for virtually the entire interval from ca. 7000 to 3500 cal. yr BP, indicating less extensive spring sea-ice conditions than at present (Vare et al., 2009; Belt et al., 2010), while melting glaciers flushed the eastern Labrador Sea with cold ice-loaded water (Solignac et al., 2011).

Southeast Greenland experienced a regional climate optimum between 5200 and 4200 cal. yr BP (Andresen et al., 2013), while a reconstruction of quantitative changes in May SIC through the Holocene on the North Iceland shelf (core MD99-2269; Justwan and Koç Karpuz, 2008) revealed low values from 5000 to 3860 cal. yr BP, a time interval with generally low April SIC off West Greenland (Fig. 8). Furthermore, Jiang et al. (2002) found that the North Iceland shelf was strongly influenced by enhanced strength of the northern branch of the IC flow around 4600–3600 cal. yr BP. This strong northern IC over the north Icelandic shelf, combined with a stronger Atlantic-water component (i.e. from the southern branch of the IC) of the WGC, indicates a generally stronger IC, which also influenced the Disko Bugt (e.g., Moros et al., 2006; Lloyd et al., 2007).

The generally warm late HTM conditions in Vaigat Strait were interrupted by an episode of markedly increased SIC values before ca. 4800 cal. yr BP (Fig. 8). This episode was also characterized by a short-term drop in warm-water diatoms (Fig. 8), indicating a short interval of decreased Atlantic water influx and cold surface-water conditions in Vaigat Strait. This change was accompanied by colder than present Arctic bottom waters, as identified by low percentages of Atlantic benthic foraminiferal assemblage and high abundances of the cold-water species *Cuneata arctica* and *Elphidium excavatum* f. *clavata* (McCarthy, 2011). Jennings et al. (2002) also identified a cooling of subsurface waters at 5000–4700 cal. yr BP off East Greenland based on the benthic foraminifera, stable isotope and IRD fluxes.

5.2. Onset of the 'Neoglacial'

Increased abundances of sea-ice diatom species, mainly *F. cylindrus* and *T. bulbosa*, as well as *B. bathyomphala* and *F. oceanica* indicate a significant increase in the influence of Polar waters in the Vaigat Strait, particularly during the intervals ca. 3700–3500, 3000–2800 and 2200–1900 cal. yr BP. Diatom-inferred SIC was high, albeit with marked fluctuations, possibly in response to an enhanced inflow of cold Polar waters during this period. This inference is supported by generally low frequencies of warm-water diatoms and Atlantic foraminifera (Fig. 8; Andresen et al., 2011). The increase in sea-ice cover was presumably a consequence of the start of the 'Neoglacial', a period of general Northern Hemispheric cooling, which started around ca. 3900 cal. yr BP in the North Atlantic region, following the climatic optimum.

At the onset of the 'Neoglacial', there was evidence of regional glacier advances in Greenland (Kelly, 1980), and both atmospheric and ocean cooling is recorded in a wide area around the eastern Labrador Sea, Baffin Bay and in East and West Greenland (e.g. Dyke et al., 1996; Dahl-Jensen et al., 1998; Kaplan et al., 2002; Seidenkrantz et al., 2007, 2008; Knudsen et al., 2008; Andresen et al., 2013; Erbs-Hansen et al., 2013), as well as in the North Atlantic (e.g. Koç Karpuz et al., 1993), although the timing of the onset of the 'Neoglacial' varies spatially across Greenland and the wider North Atlantic region (e.g. Kaufman et al., 2004).

A similar scenario was recognized in Disko Bugt, where both diatoms and lithological and benthic foraminiferal data record relatively cool conditions during the time interval 3500–2000 cal. yr BP (Moros et al., 2006; Lloyd et al., 2007). Likewise, in Ameralik fjord near Nuuk, a multiproxy study indicated a decreased influx of WGC water at subsurface depths (Seidenkrantz et al., 2007).

To the north, in the central Canadian Arctic Archipelago, elevated IP_{25} values indicated relatively more intensive spring sea-ice occurrences, beginning at ca. 3500–3000 cal. yr BP (Vare et al., 2009; Belt et al., 2010). Furthermore, the disappearance of calcarous foraminifera in northernmost Baffin Bay at ca. 3000 cal yrs BP (Knudsen et al., 2008), as well as a generally longer sea-ice season after 3600 cal. yr BP (Levac et al., 2001), indicated a decreased surface water temperature in that area. The cooling also resulted in decreased glacier melting (Fisher et al., 1995) and reduced transport of meltwater and sea ice with the Labrador Current (Solignac et al., 2011).

Moreover, the clear correspondence between the April SIC in Disko Bugt and May SIC on the North Iceland shelf during this interval (Fig. 8) suggests that the IC decreased in strength, and that an enhanced inflow of Polar water from the EGC affected the hydrography and climate in both areas. Marine archives from East and Southeast Greenland also show that the Neoglacial interval was cold and variable after 3500 cal. yr BP, with decreased influence of Atlantic-source water and increased freshwater forcing from the Arctic Ocean, advance of the Greenland Ice Sheet and a southward shift of the Polar Front (Jennings et al., 2011; Andresen et al., 2013) causing a shift towards a more meridional atmospheric circulation bringing cold air from the north (Jessen et al., 2011).

Studies of the terrestrial environment in the Greenland region also show a general cooling after ca. 4000–3500 cal. yr BP (e.g. Weidick et al., 1990, 2004; Eisner et al., 1995; Kerwin et al., 2004). In southern Greenland, a marked cooling was recorded in a lake sediment record from Angissoq Island after 3700 cal. yr BP (Andresen et al., 2004), and in the Kangerlussuaq region, Anderson et al. (1999) dated the onset of the 'Neoglacial' to 3950 cal. yr BP, based on lithological features of a lake core.

5.3. Roman warm period

Low values of SIC indicate a generally decreased sea-ice cover between 1900 and 1510 cal. yr BP, when the diatoms were characterized by a marked increase in warm-water species and near absence of the sea-ice species *F. arctica* and *T. bulbosa*. This suggests a period of enhanced influence of relatively warm Atlantic water into Vaigat Strait and a strong sea-ice reduction in that interval, corresponding in time to the later part of the 'Roman Warm Period' of mainland Europe.

However, during the early part of the 'Roman Warm Period', there was a short-term increase in sea-ice cover, coinciding with the decline of warm-water diatoms and Atlantic-water foraminiferal species (Fig. 8).

An episode of increased surface-water temperature and a warmer/stronger WGC was recognized in Disko Bugt between 2200/2000 and 1500/1400 cal. yr BP based on diatoms, benthic foraminifera and dinoflagellate cysts in cores DA00-02P and DA00-03P (Moros et al., 2006; Lloyd et al., 2007; Seidenkrantz et al., 2008). Also, on the East Greenland shelf, benthic foraminiferal data indicated relatively warmer waters at ca. 2000–1500 cal. yr BP, presumably as a result of a weakening of the EGC (Jennings et al., 2002), a result which is supported by foraminiferal data from Igaliku fjord in South Greenland (Lassen et al., 2004) and from Holsteinsborg Dyb by Erbs-Hansen et al. (2013). A weakening of the EGC would result in a relative increase in the influence of the IC component of the WGC and decreased sea-ice cover. Further evidence of this warming has also been demonstrated by low values of reconstructed May SIC on the North Iceland shelf, by high solar irradiance (Fig. 8) and by lower IP_{25} fluxes, as well as the reoccurrence of bowhead whale remains the central Canadian Arctic Archipelago during the time interval 2000–1500 cal. yr BP (Belt et al., 2010). On the other hand, subsurface waters seem to have cooled in the Nuuk area, indicating that here the warm water of the IC, and the WGC in general, did not reach the coastal region (Seidenkrantz et al., 2007).

Based on these studies, it is suggested that the general northward heat transport via the North Atlantic Current increased during the Roman Warm Period. This warming may have moved northward along West Greenland at some distance from the coast before reaching the Disko Bugt region, where it also influenced surface water conditions and caused diminished sea-ice cover.

5.4. Post-1510 cal. yr BP

The variations in SIC after 1510 ca. yr BP appear to be closely related to the historical climate periods recognized in Europe (cf. Lamb, 1995), and these time intervals are therefore described separately in the following section.

5.4.1. Dark Ages cold period

Between 1510 and 1120 cal. yr BP, there was a significant increase in the sea-ice species *F. cylindrus* and a marked decline, or even disappearance, of warm-water diatom taxa coinciding with the extensive sea-ice cover indicated by the SIC reconstruction (Fig. 8). This implies that the influence of cold Polar waters in the Vaigat Strait increased and further led to enhanced sea-ice cover during this period.

The inferences about SIC implied by the diatoms are supported by dinoflagellate cyst data from DA00-02 in Disko Bugt, which show a gradual decrease in warm-water taxa from 1500 to 1300 cal. yr BP (Seidenkrantz et al., 2008), and by diatom and dinoflagellate cyst records from South Greenland, indicating a cold phase related to the influence of the EGC (Jensen et al., 2004; Roncaglia and Kuijpers, 2004), although the overall strength of the WGC seems to have increased (cf. Seidenkrantz et al., 2007). In addition, the reconstructed May SIC on the North Iceland shelf indicates increased influx of cold Polar waters during this interval (Fig. 8). At this time, NW Europe was characterized by a significant climatic deterioration known as the 'Dark Ages Cold Period' (DACP, ca. 1550–1150 cal. yr BP; cf. Lamb, 1995). The indication of relatively high SIC and cold climate at the core site DA06-139G during this time interval coincides with a period of low solar irradiance (Fig. 8).

5.4.2. Medieval climate anomaly

Low abundance of sea-ice diatoms and the reappearance of warm-water species, reaching almost the same level as in zone I (later part of the HTM, 5000–3860 cal. yr BP), indicate a short-lived high influx of Atlantic surface waters both to the Vaigat Strait and to the North Icelandic shelf (Fig. 8) during the time period 1120–650 cal. yr BP, corresponding in time to the 'Medieval Climate Anomaly' (MCA). Evidence of the MCA can be found throughout West Greenland and across the North Atlantic region. In Holsteinsborg Dyb, off West Greenland, the MCA is documented by relatively warm surface waters during the time interval 1150–650 cal. yr BP (Sha et al., 2012). In Igaliku Fjord, Southwest Greenland, Jensen et al. (2004) identified a period of reduced sea ice from 1180 to 600 cal. yr BP associated with a decrease in the influx of EGC waters, and Roncaglia and Kuijpers (2004) found a considerable reduction of the seasonal sea-ice cover based on dinoflagellate cysts during the interval 990–665 cal. yr BP.

On the other hand, diatom and dinoflagellate cyst data from the central and western Disko Bugt suggest that this area experienced very low sea-surface temperatures and a decrease in Atlantic water influx from around 1300 cal. yr BP (Moros et al., 2006; Seidenkrantz et al., 2008; Ribeiro et al., 2012), as well as reduced meltwater release, indicating that the warmer water masses did not influence the surface waters of the area until they reached the north-eastern Disko Bugt, nor did they reach the coastal regions of West Greenland (Seidenkrantz et al., 2007).

On the East Greenland shelf between 1200 and 850 cal. yr BP, the influence of the Polar water was reduced which allowed the encroachment of Atlantic Intermediate Water along the sea floor (Jennings and Weiner, 1996). Also, the North Icelandic shelf was dominated by the influence of Atlantic water during 1150–650 cal. yr BP (e.g. Eiríksson et al., 2000; Jiang et al., 2002; Knudsen et al., 2004, 2012; Ran et al., 2011). Similarly, diatom records from the central Canadian Arctic Archipelago reveal a higher species diversity around ca. 1150–600 cal. yr BP, suggest a warmer climate than before and after (LeBlanc et al., 2004). In addition, reconstruction of late-summer Arctic sea-ice cover from high-resolution terrestrial proxies for the circum-Arctic region suggests that a pronounced decline in summer Arctic sea-ice cover occurred before 750 cal. yr BP, coinciding with the MCA (Kinnard et al., 2011).

5.4.3. Little Ice Age

Warm-water diatom taxa were almost completely absent after 650 cal. yr BP in core DA06-139G, whereas sea-ice species became abundant. The April SIC reconstruction for the period after ca. 650 cal. yr BP showed much higher values than previously, suggesting that this increase in the SIC was driven by a strengthening in the inflow of cold Polar water from the EGC. Although the temporal range of the so-called 'Little Ice Age' (LIA) is not particularly well-defined in the Northern Hemisphere (Grove, 1988, 2001; Broecker, 2000) and appears to be influenced significantly by location (Mayewski et al., 2004), the interval of enhanced sea-ice cover after 650 cal. yr BP in our record coincided broadly with the general timing of the LIA. As relatively warm, saline Atlantic surface water in Vaigat Strait was replaced by cold, low-salinity Polar water, it became more susceptible to sea-ice formation.

A change to colder hydrographic conditions, caused by increased inflow of Arctic water to the central Disko Bugt, was also indicated by the occurrence of glaciomarine foraminiferal faunas after ca. 500 cal. yr BP (Lloyd, 2006a). Evidence of extended sea-ice cover in Disko Bugt was reported by Ribeiro et al. (2012: Fig. 5) after 450 cal. yr BP, although Seidenkrantz et al. (2008) found that surface-water conditions did not cool further or may even have become slightly warmer in that area during the LIA than during the MCA. Cold conditions, as well as persistent sea-ice cover, were also described for the LIA both for the West Greenland shelf (Sha et al., 2012) and Southwest Greenland (Jensen et al., 2004; Roncaglia and Kuijpers, 2004).

Offshore Southeast Greenland, diatom data suggested a cooling of the EGC after ca. 750 cal. yr BP (Jensen, 2003), coinciding with similar indication from onshore data in the same area (Wagner et al., 2000). Furthermore, a diatom-based SST reconstruction from the North Icelandic shelf indicated a marked decrease in temperature at around 650 cal. yr BP (Jiang et al., 2005), caused by a relatively high influence of Polar waters from the EGC to that area. After 750 cal. yr BP, the elevated IP_{25} values from the same core indicate the occurrence of sea ice along the North Icelandic coast during winter and spring, reflecting

sea-ice advection/drift out of the Arctic (Massé et al., 2008; Kinnard et al., 2011).

The similarity between the reconstructed April SIC off West Greenland and the May SIC on the North Iceland shelf suggested that a strong influence of Polar waters, which was also reflected on the North Iceland shelf, would result in permanent sea-ice conditions as relatively colder water masses of the WGC flows into Disko Bugt during the LIA. This would potentially create a strong stratification between the polar surface waters and the warmer Atlantic-source subsurface waters seen in records along the West Greenland coast and parts of East Greenland (Seidenkrantz et al., 2007, 2008; Andresen et al., 2013; Erbs-Hansen et al., 2013). This change was suggested to be linked to a negative North Atlantic Oscillation-type scenario and a contracted Subpolar Gyre (Seidenkrantz et al. 2007, 2008; Andresen et al., 2013). In summary, for the period after 1500 cal. yr BP, the reconstructed SIC suggests that Vaigat Strait experienced a warmer period of reduced sea-ice cover and two cold intervals, with the most extensive sea-ice cover indicated during the LIA.

5.5. Implications of palaeo-sea-ice conditions

The diatom results suggest that sea-ice conditions in Disko Bugt are strongly influenced by changes in the relative strengths of the two components of the WGC, the cold Polar water from the EGC and the relatively warm Atlantic water from the IC. Thus, high values of April SIC generally correspond to low abundances of warm-water diatoms and vice versa. Particularly high SIC values were recorded during the time interval 1510–1120 cal. yr BP and after 650 cal. yr BP (Fig. 8).

Similarly, on the North Icelandic shelf, the inferred May SIC record was influenced by both the IC and the EGC (Justwan and Koç Karpuz, 2008), and the distribution pattern is similar to that found in the Disko Bugt, particularly during the time periods before 3500 cal. yr BP and after 2000 cal. yr BP (Fig. 8). Additionally, in two sediment cores obtained beneath the sea-ice bearing Polar Water of the EGC on the Southeast Greenland shelf, Jennings et al. (2011) found that the IC penetrated further north between 6800 and 3500 cal. yr BP than observed in recent decades. Furthermore, they reported a Neoglacial interval (beginning at 3500 cal. yr BP), which was cold and variable with a relatively thick and extensive Polar water cover and with considerably diminished northward advection of the IC. Similar shifts in the strength of the IC and the EGC have been reported from more coastal waters at Sermilik Fjord in East Greenland (Andresen et al., 2013).

In summary, these results suggest that on longer time scales, changes in the relative strength of the two components of the WGC (e.g. the IC and the EGC waters) in Disko Bugt and in other North Atlantic regions under the influence of these water masses (e.g. the Southeast Greenland shelf and the North Icelandic shelf) were generally synchronous. Hence, severe sea-ice conditions in Disko Bugt may be caused by relatively stronger EGC influx to the WGC.

There is some agreement between the reconstructed SIC record and total solar irradiance variations, in particular after 1500 cal. yr BP, indicating that solar forcing may also be one of the forcing mechanisms behind the palaeo-sea-ice changes (Fig. 8). Braun et al. (2005) suggested that the North Atlantic region is particularly sensitive to solar forcing. While variations in the atmospheric heat fluxes can trigger shifts of the sea-ice margin that result in evaporation anomalies, because of the insulating effect of sea ice (Lohmann and Gerdes, 1998), solar forcing can cause meltwater anomalies due to its effect on the mass balance of the ice sheets surrounding this region.

Several studies have demonstrated that the effect of solar changes on the regional modes of atmospheric variability is evident in the instrumental record (Kodera and Kuroda, 2002; Ruzmaikin et al., 2004; Haigh and Roscoe, 2006). Thus, the strong correlation of the Norwegian Sea temperature with solar activity over the last millennium indicates that variations in solar activity affect the regional modes of atmospheric variability which, in turn, control the poleward transport and temperature of warm Atlantic surface waters (Sejrup et al., 2010). Furthermore, Bond et al. (2001) concluded that peak volumes of Holocene drift ice resulted from southward expansions of polar waters coincided with times of reduced solar output. As a result, a large amount of multi-year ice originating from the Arctic Ocean periodically entered West Greenland waters.

A sea-ice thermodynamic model (Schramm et al., 1997; Bitz and Roe, 2004; Tedesco et al., 2009; Goosse et al., 2013) computes the heat balance at the interfaces with the ocean and the atmosphere, the sea-ice melting/formation, and assumes that sea-ice freezing and melting are primarily influenced by solar radiation and heat exchange with the atmosphere and ocean (Schramm et al., 1997).

6. Conclusions

Modern diatom assemblages from 72 surface sediment samples from west of Greenland and around Iceland were combined with the passive microwave sea-ice data in order to establish a diatom-based transfer function for reconstructing sea-ice concentration (SIC). A Canonical correspondence analysis (CCA) indicated that April SIC is the most important environmental factor controlling the distribution of diatoms in the area, and this parameter is therefore potentially reconstructable.

In order to test the validity of the diatom-based SIC transfer function, April SIC for the last ~75 yr was reconstructed by using diatom data from box core GA306-BC4 off West Greenland. A general consistency between the reconstructed SIC and the satellite and modelled sea-ice records supports the reliability of the diatom-based April SIC reconstruction as a measure for studying palaeoceanographic changes in the Disko Bugt during the last 5000 yr.

Diatom data from Vaigat Strait (DA06-139G) reflect changes in climate and oceanography during the last 5000 yr and six diatom assemblage zones were established. The main changes in the diatom assemblage zones were related to inflow proportions of the two components of the West Greenland Current (WGC), i.e. the cold East Greenland Current and the relatively warm Irminger Current, into Baffin Bay and Labrador Sea.

The diatom SIC reconstruction showed that the April SIC varied between 25 and 95% over the last 5000 yr. Generally low SIC before 3860 cal. yr BP, except for a short period around 4900 cal. yr BP, suggests a relatively warm period, corresponding in time to the latest part of the Holocene Thermal Maximum. The April SIC oscillated around the mean value (55%) between 3860 and 1510 cal. yr BP with relatively high inferred values at ca. 3700–3500, 3000–2800 and 2200–1900 cal. yr BP. After ca. 1510 cal. yr BP, the April SIC was much higher than earlier, particularly so after ca. 650 cal. yr BP, indicating extensive sea-ice cover during the Little Ice Age.

Agreement between changes in the reconstructed April SIC and variations in abundances of the main diatom components suggests that sea-ice conditions in Disko Bugt were generally strongly influenced by changes in strength of the transport of Atlantic vs. Polar water via the WGC. In addition, the agreement between the reconstructed SIC record and total solar irradiance, suggests that solar forcing may also be one of the important contributors to the sea-ice changes.

Acknowledgements

Core DA06-139G was collected in 2006 during a cruise of RV *Dana* funded by GEUS, the Bureau of Mineral Resources in Nuuk, and NunaOil, Greenland. We thank the captain and crew for their engagement during the work at sea, and John Boserup (GEUS) for assisting with sediment coring. Kaarina Weckström and Camilla S. Andresen are also acknowledged for sharing their data. We acknowledge the financial supports from the National Natural Science Foundation of China (grants 41176048, 40976115), International cooperation project of Chinese Arctic and Antarctic Administration, SOA (grant IC201309) and 111 project (B08022).

This paper is also a contribution to the Danish Council for Independent Research, Natural Sciences (FNU) projects "Green-Ice" (09-072321), "TROPOLINK" (09-069833) and OCEANHEAT (12-126709). The research leading to these results has received funding from the European Union's Seventh Framework programme (FP7/2007-2013) under grant agreement no. 243908, 'Past4uture', Climate change – Learning from the past climate. This is Past4Future contribution no.72. Finally, we are grateful to two anonymous referees and the Editor, Prof. Finn Surlyk for the constructive and useful comments, and to Prof. John Anderson for the constructive suggestions and correction of the English text.

Appendix A. Supplementary data

Supplementary data to this article can be found online at http://dx.doi.org/10.1016/j.palaeo.2014.03.028.

References

Andersen, O.G.N., 1981a. The annual cycle of phytoplankton of primary production and hyrdrography in the Disko Bugt area, West Greenland. Medd. Grønland 218, 1–68.
Andersen, O.G.N., 1981b. The annual cycle of temperature, salinity, currents and water masses in Disko Bugt and adjacent waters, West Greenland. Medd. Grønland 217, 1–36.
Anderson, N.J., Bennike, O., Christoffersen, K., Jeppesen, E., Markager, S., Miller, G., Renberg, I., 1999. Limnological and palaeolimnological studies of lakes in southwestern Greenland. Geol. Green. Surv. Bull. 183, 68–74.
Andresen, C.S., Björck, S., Bennike, O., Bond, G., 2004. Holocene climate changes in southern Greenland: evidence from lake sediments. J. Quat. Sci. 19, 783–795.
Andresen, C.S., McCarthy, D.J., Dylmer, C.V., Seidenkrantz, M.-S., Kuijpers, A., Lloyd, J.M., 2011. Interaction between subsurface ocean waters and calving of the Jakobshavn Isbræ during the late Holocene. The Holocene 21, 211–224.
Andresen, C.S., Hansen, M.J., Seidenkrantz, M.-S., Jennings, A.E., Knudsen, M.F., Nørgaard-Pedersen, N., Larsen, N.K., Kuijpers, A., Pearce, C., 2013. Mid- to late-Holocene oceanographic variability on the Southeast Greenland shelf. The Holocene 23, 167–178.
Bauch, H.A., Polyakova, Y.I., 2000. Late Holocene variations in Arctic shelf hydrology and sea-ice regime: evidence from north of the Lena Delta. Int. J. Earth Sci. 89, 569–577.
Belt, S.T., Vare, L.L., Massé, G., Manners, H.R., Price, J.C., MacLachlan, S.E., Andrews, J.T., Schmidt, S., 2010. Striking similarities in temporal changes to spring sea ice occurrence across the central Canadian Arctic Archipelago over the last 7000 years. Quat. Sci. Rev. 29, 3489–3504.
Birks, H.J.B., 1995. Quantitative paleoenvironmental reconstructions. In: Maddy, D., Brew, J.S. (Eds.), Statistical modelling of Quaternary Science Data Technical Guide 5. Quaternary Research Association, Cambridge, pp. 161–254.
Birks, H.J.B., 1998. Numerical tools in palaeolimnology — Progress, potentialities, and problems. J. Paleolimnol. 20, 307–332.
Bitz, C.M., Roe, G.H., 2004. A mechanism for the high rate of sea ice thinning in the Arctic Ocean. J. Clim. 17, 3623–3632.
Bond, G., Kromer, B., Beer, J., Muscheler, R., Evans, M.N., Showers, W., Hoffmann, S., Lotti-Bond, R., Hajdas, I., Bonani, G., 2001. Persistent solar influence on North Atlantic climate during the Holocene. Science 294, 2130–2136.
Braun, H., Christl, M., Rahmstorf, S., Ganopolski, A., Mangini, A., Kubatzki, C., Roth, K., Kromer, B., 2005. Possible solar origin of the 1,470-year glacial climate cycle demonstrated in a coupled model. Nature 438, 208–211.
Broecker, W.S., 2000. Was a change in thermohaline circulation responsible for the Little Ice Age? Proc. Natl. Acad. Sci. U. S. A. 97, 1339–1342.
Buch, E., 2000. A monograph on the physical oceanography of the Greenland waters. Danish Meteorological Institute Scientific Report, Copenhagen pp. 1–405.
Buch, E., 2002. Present Oceanographic Conditions in Greenland Waters. Danish Meteorological Institute Scientific Report, Copenhagen pp. 1–36.
Buch, E., Pedersen, S.A., Ribergaard, M.H., 2004. Ecosystem Variability in West Greenland Waters. J. Northwest Atl. Fish. Sci. 34, 13–28.
Cavalieri, D., Parkinson, C., Gloersen, P., Zwally, H.J., 1996. Sea Ice Concentrations from Nimbus-7 SMMR and DMSP SSM/I-SSMIS Passive Microwave Data. National Snow and Ice Data Center, Boulder, Colorado USA.
Cremer, H., 1999. Distribution patterns of diatom surface sediment assemblages in the Laptev Sea (Arctic Ocean). Mar. Micropaleontol. 38, 39–67.
Crosta, X., Pichon, J.J., Burckle, L.H., 1998. Application of modern analog technique to marine antarctic diatoms: reconstruction of maximum sea-ice extent at the last glacial maximum. Paleoceanography 13, 284–297.
Crosta, X., Sturm, A., Armand, L., Pichon, J.-J., 2004. Late Quaternary sea ice history in the Indian sector of the Southern Ocean as recorded by diatom assemblages. Mar. Micropaleontol. 50, 209–223.
Dahl-Jensen, D., Mosegaard, K., Gundestrup, N., Clow, G.D., Johnsen, S.J., Hansen, A.W., Balling, N., 1998. Past temperatures directly from the Greenland Ice Sheet. Science 282, 268–271.
Dalhoff, F., Kuijpers, A., 2007. Havbunds prøveindsamling ud for Vest Grønland 2006. RV Dana Cruise report., Danmarks og Grønlands Geologiske Undersøgelse Rapport, pp. 1–51.
De Sève, M.A., 1999. Transfer function between surface sediment diatom assemblages and sea-surface temperature and salinity of the Labrador Sea. Mar. Micropaleontol. 36, 249–267.
De Sève, M.A., Dunbar, M.J., 1990. Structure and composition of ice algal assemblages from the Gulf of St. Lawrence, Magdalen Islands area. Can. J. Fish. Aquat. Sci. 47, 780–788.
de Vernal, A., Hillaire-Marcel, C., 2000. Sea-ice cover, sea-surface salinity and halo-/thermocline structure of the northwest North Atlantic: modern versus full glacial conditions. Quat. Sci. Rev. 19, 65–85.
de Vernal, A., Hillaire-Marcel, C., 2006. Provincialism in trends and high frequency changes in the northwest North Atlantic during the Holocene. Glob. Planet. Chang. 54, 263–290.
de Vernal, A., Eynaud, F., Henry, M., Hillaire-Marcel, C., Londeix, L., Mangin, S., Matthiessen, J., Marret, F., Radi, T., Rochon, A., Solignac, S., Turon, J.L., 2005. Reconstruction of sea-surface conditions at middle to high latitudes of the Northern Hemisphere during the Last Glacial Maximum (LGM) based on dinoflagellate cyst assemblages. Quat. Sci. Rev. 24, 897–924.
de Vernal, A., Gersonde, R., Goosse, H., Seidenkrantz, M.-S., Wolff, E.W., 2013a. Sea ice in the paleoclimate system: the challenge of reconstructing sea ice from proxies — an introduction. Quat. Sci. Rev. 79, 1–8.
de Vernal, A., Hillaire-Marcel, C., Rochon, A., Fréchette, B., Henry, M., Solignac, S., Bonnet, S., 2013b. Dinocyst-based reconstructions of sea ice cover concentration during the Holocene in the Arctic Ocean, the northern North Atlantic Ocean and its adjacent seas. Quat. Sci. Rev. 79, 111–121.
de Vernal, A., Rochon, A., Fréchette, B., Henry, M., Radi, T., Solignac, S., 2013c. Reconstructing past sea ice cover of the Northern Hemisphere from dinocyst assemblages: status of the approach. Quat. Sci. Rev. 79, 122–134.
Drinkwater, K.F., 1996. Atmospheric and oceanic variability in the Northwest Atlantic during the 1980s and early 1990s. J. Northwest Atl. Fish. Sci. 18, 77–97.
Dyke, A.S., Dale, J.E., McNeely, R.N., 1996. Marine molluscs as indicators of environmental change in glaciated North America and Greenland during the last 18 000 years. Géog. Phys. Quatern. 50, 125–184.
Eiríksson, J., Knudsen, K.L., Haflidason, H., Henriksen, P., 2000. Late-glacial and Holocene palaeoceanography of the North Icelandic shelf. J. Quat. Sci. 15, 23–42.
Eisner, W.R., Törnqvist, T.E., Koster, E.A., Bennike, O., van Leeuwen, J.F.N., 1995. Paleoecological studies of a Holocene Lacustrine Record from the Kangerlussuaq (Søndre Strømfjord) Region of West Greenland. Quat. Res. 43, 55–66.
Erbs-Hansen, D.R., Knudsen, K.L., Jesper Olsen, J., Lykke-Andersen, H., Underbjerg, J.A., Sha, L., 2013. Paleoceanographical development off Sisimiut, West Greenland, during the last 7000 years: a multiproxy study. Mar. Micropaleontol. 102, 79–97.
Fisher, D.A., Koerner, R.M., Reeh, N., 1995. Holocene climatic records from Agassiz Ice Cap, Ellesmere Island, NWT, Canada. The Holocene 5, 19–24.
Gersonde, R., Crosta, X., Abelmann, A., Armand, L., 2005. Sea-surface temperature and sea ice distribution of the Southern Ocean at the EPILOG Last Glacial Maximum—a circum-Antarctic view based on siliceous microfossil records. Quat. Sci. Rev. 24, 869–896.
Goosse, H., Roche, D.M., Mairesse, A., Berger, M., 2013. Modelling past sea ice changes. Quat. Sci. Rev. 79, 191–206.
Grimm, E.C., 1987. Coniss: a fortran 77 program for stratigraphically constrained cluster analysis by the method of incremental sum of squares. Comput. Geosci. 13, 13–35.
Grove, J.M., 1988. The Little Ice Age. Routledge, New York.
Grove, J.M., 2001. The initiation of the "Little Ice Age" in regions round the North Atlantic. Clim. Chang. 48, 53–82.
Haigh, J.D., Roscoe, H.K., 2006. Solar influences on polar modes of variability. Meteorol. Z. 15, 371–378.
Håkansson, H., 1984. The recent diatom succession of Lake Havgårdssjön, South Sweden. In: Mann, D.G. (Ed.), Proceedings of the Seventh International Diatom Symposium. Otto Koeltz Science Publishers, Koenigstein, pp. 411–429.
Hansen, K.Q., Buch, E., Gregersen, U., 2004. Weather, Sea and Ice Conditions Offshore West Greenland – Focusing on New License Areas 2004. Danish Meteorological Institute Scientific Report, Copenhagen pp. 1–31.
Hasle, G.R., Syvertsen, E.E., 1997. Marine diatoms. In: Tomas, C.R. (Ed.), Identifying Marine Phytoplankton. Academic Press, San Diego, pp. 5–385.
Jennings, A.E., Weiner, N.J., 1996. Environmental change in eastern Greenland during the last 1300 years: evidence from foraminifera and lithofacies in Nansen Fjord, 68°N. The Holocene 6, 179–191.
Jennings, A.E., Knudsen, K.L., Hald, M., Hansen, C.V., Andrews, J.T., 2002. A mid-Holocene shift in Arctic sea-ice variability on the East Greenland Shelf. The Holocene 12, 49–58.
Jennings, A., Andrews, J., Wilson, L., 2011. Holocene environmental evolution of the SE Greenland Shelf North and South of the Denmark Strait: Irminger and East Greenland current interactions. Quat. Sci. Rev. 30, 980–998.
Jensen, K.G., 2003. Holocene hydrographic changes in Greenland coastal waters: reconstructing environmental change from sub-fossil and contemporary diatoms. Geological Survey of Greenland and Denmark, Copenhagen pp. 1–160.
Jensen, K.G., Kuijpers, A., Koç Karpuz, N., Heinemeier, J., 2004. Diatom evidence of hydrographic changes and ice conditions in Igaliku Fjord, South Greenland, during the past 1500 years. The Holocene 14, 152–164.
Jessen, C.A., Solignac, S., Nørgaard-Pedersen, N., Mikkelsen, N., Kuijpers, A., Seidenkrantz, M.-S., 2011. Exotic pollen as an indicator of variable atmospheric circulation over the Labrador Sea region during the mid to late Holocene. J. Quat. Sci. 26, 286–296.
Jiang, H., Seidenkrantz, M.-S., Knudsen, K.L., Eiríksson, J., 2001. Diatom surface sediment assemblages around Iceland and their relationships to oceanic environmental variables. Mar. Micropaleontol. 41, 73–96.
Jiang, H., Seidenkrantz, M.-S., Knudsen, K.L., Eiríksson, J., 2002. Late-Holocene summer sea-surface temperatures based on a diatom record from the north Icelandic shelf. The Holocene 12, 137–147.

Jiang, H., Eiríksson, J., Schulz, M., Knudsen, K.L., Seidenkrantz, M.-S., 2005. Evidence for solar forcing of sea-surface temperature on the North Icelandic Shelf during the late Holocene. Geology 33, 73–76.
Justwan, A., Koç Karpuz, N., 2008. A diatom based transfer function for reconstructing sea ice concentrations in the North Atlantic. Mar. Micropaleontol. 66, 264–278.
Kaplan, M.R., Wolfe, A.P., Miller, G.H., 2002. Holocene environmental variability in Southern Greenland inferred from lake sediments. Quat. Res. 58, 149–159.
Katsuki, K., Takahashi, K., 2005. Diatoms as paleoenvironmental proxies for seasonal productivity, sea-ice and surface circulation in the Bering Sea during the late Quaternary. Deep-Sea Res. II Top. Stud. Oceanogr. 52, 2110–2130.
Kaufman, D.S., Ager, T.A., Anderson, N.J., Anderson, P.M., Andrews, J.T., Bartlein, P.J., Brubaker, L.B., Coats, L.L., Cwynar, L.C., Duvall, M.L., Dyke, A.S., Edwards, M.E., Eisner, W.R., Gajewski, K., Geirsdóttir, A., Hu, F.S., Jennings, A.E., Kaplan, M.R., Kerwin, M.W., Lozhkin, A.V., MacDonald, G.M., Miller, G.H., Mock, C.J., Oswald, W.W., Otto-Bliesner, B.L., Porinchu, D.F., Rühland, K., Smol, J.P., Steig, E.J., Wolfe, B.B., 2004. Holocene thermal maximum in the western Arctic (0–180°W). Quat. Sci. Rev. 23, 529–560.
Kelly, M., 1980. The status of the Neoglacial in western Greenland. Grønl. Geol. Unders. Rapp. 96, 1–24.
Kerwin, M.W., Overpeck, J.T., Webb, R.S., Anderson, K.H., 2004. Pollen-based summer temperature reconstructions for the eastern Canadian boreal forest, subarctic, and Arctic. Quat. Sci. Rev. 23, 1901–1924.
Kinnard, C., Zdanowicz, C.M., Fisher, D.A., Isaksson, E., de Vernal, A., Thompson, L.G., 2011. Reconstructed changes in Arctic sea ice over the past 1,450 years. Nature 479, 509–512.
Knudsen, K.L., Eiríksson, J., Jansen, E., Jiang, H., Rytter, F., Gudmundsdóttir, E.R., 2004. Palaeoceanographic changes off North Iceland through the last 1200 years: foraminifera, stable isotopes, diatoms and ice rafted debris. Quat. Sci. Rev. 23, 2231–2246.
Knudsen, K.L., Stabell, B., Seidenkrantz, M.-S., Eiríksson, J., Blake Jr., W., 2008. Deglacial and Holocene conditions in northernmost Baffin Bay: sediments, foraminifera, diatoms and stable isotopes. Boreas 37, 346–376.
Knudsen, K.L., Eiríksson, J., Bartels-Jónsdóttir, H.B., 2012. Oceanographic changes through the last millennium off North Iceland: temperature and salinity reconstructions based on foraminifera and stable isotopes. Mar. Micropaleontol. 84–85, 54–73.
Koç Karpuz, N., Schrader, H., 1990. Surface sediment diatom distribution and Holocene Paleotemperature variations in the Greenland, Iceland and Norwegian Sea. Paleoceanography 5, 557–580.
Koç Karpuz, N., Jansen, E., Haflidason, H., 1993. Paleoceanographic reconstructions of surface ocean conditions in the Greenland, Iceland and Norwegian seas through the last 14 ka based on diatoms. Quat. Sci. Rev. 12, 115–140.
Kodera, K., Kuroda, Y., 2002. Dynamical response to the solar cycle. J. Geophys. Res. 107, 4749.
Krawczyk, D., Witkowski, A., Moros, M., Lloyd, J., Kuijpers, A., Kierzek, A., 2010. Late-Holocene diatom-inferred reconstruction of temperature variations of the West Greenland Current from Disko Bugt, central West Greenland. The Holocene 20, 659–666.
Krebs, W.N., 1983. Ecology of neritic marine diatoms, Arthur Harbor, Antarctica. Micropaleontology 29, 267–297.
Lamb, H.H., 1995. Climate, History and the Modern World. Routledge, New York.
Lassen, S.J., Kuijpers, A., Kunzendorf, H., Hoffmann-Wieck, G., Mikkelsen, N., Konradi, P., 2004. Late-Holocene Atlantic bottom-water variability in Igaliku Fjord, South Greenland, reconstructed from foraminifera faunas. The Holocene 14, 165–171.
LeBlanc, M., Gajewski, K., Hamilton, P.B., 2004. A diatom-based Holocene palaeoenvironmental record from a mid-arctic lake on Boothia Peninsula, Nunavut, Canada. The Holocene 14, 417–425.
LeDrew, E., Barber, D.C., Agnew, T., Dunlop, D., 1992. Canadian sea ice atlas from microwave remotely sensed imagery, July 1987 to June 1990, Ottawa.
Levac, E., Vernal, A.D., Blake Jr., W., 2001. Sea-surface conditions in northernmost Baffin Bay during the Holocene: palynological evidence. J. Quat. Sci. 16, 353–363.
Lloyd, J.M., 2006a. Late Holocene environmental change in Disko Bugt, west Greenland: interaction between climate, ocean circulation and Jakobshavn Isbrae. Boreas 35, 35–49.
Lloyd, J.M., 2006b. Modern distribution of Benthic Foraminifera from Disko Bugt, West Greenland. J. Foraminifer. Res. 36, 315–331.
Lloyd, J.M., Kuijpers, A., Long, A., Moros, M., Park, L.A., 2007. Foraminiferal reconstruction of mid- to late-Holocene ocean circulation and climate variability in Disko Bugt, West Greenland. The Holocene 17, 1079–1091.
Lloyd, J., Moros, M., Perner, K., Telford, R.J., Kuijpers, A., Jansen, E., McCarthy, D., 2011. A 100 yr record of ocean temperature control on the stability of Jakobshavn Isbrae, West Greenland. Geology 39, 867–870.
Lohmann, G., Gerdes, R., 1998. Sea ice effects on the sensitivity of the thermohaline circulation in simplified atmosphere–ocean-sea ice models. J. Clim. 11, 2789–2803.
Long, A.J., Roberts, D.H., 2003. Late Weichselian deglacial history of Disko Bugt, West Greenland, and the dynamics of the Jakobshavns Isbrae ice stream. Boreas 32, 208–226.
Massé, G., Rowland, S.J., Sicre, M.-A., Jacob, J., Jansen, E., Belt, S.T., 2008. Abrupt climate changes for Iceland during the last millennium: evidence from high resolution sea ice reconstructions. Earth Planet. Sci. Lett. 269, 565–569.
Mayewski, P.A., Rohling, E.E., Stager, J.C., Karlén, W., Maasch, K.A., Meeker, L.D., Meyerson, E.A., Gasse, F., van Kreveld, S., Holmgren, K., Lee-Thorp, J.A., Rosqvist, G., Rack, F., Staubwasser, M., Schneider, R.R., Steig, E.J., 2004. Holocene climate variability. Quat. Res. 62, 243–255.
McCarthy, D.J., 2011. Late Quaternary Ice-ocean Interactions in Central West Greenland. Durham University, Durham pp. 1–310.
McNeely, R., Dyke, A.S., Southon, J.R., 2006. Canadian marine reservoir ages, preliminary data assessment. Geol. Surv. Can. 3 (Open File 5049).
Medlin, L.K., Priddle, J., 1990. Polar Marine Diatoms. Natural Environment Research Council, Cambridge.
Miller, G.H., Geirsdóttir, Á., Koerner, R.M., 2001. Climate implications of changing Arctic sea ice. EOS Trans. Am. Geophys. Union 82, 97–103.
Møller, H.S., Jensen, K.G., Kuijpers, A., Aagaard-Sørensen, S., Seidenkrantz, M.-S., Prins, M., Endler, R., Mikkelsen, N., 2006. Late-Holocene environment and climatic changes in Ameralik Fjord, southwest Greenland: evidence from the sedimentary record. The Holocene 16, 685–695.
Moros, M., Jensen, K.G., Kuijpers, A., 2006. Mid- to late-Holocene hydrological and climatic variability in Disko Bugt, central West Greenland. The Holocene 16, 357–367.
Müller, J., Wagner, A., Fahl, K., Stein, R., Prange, M., Lohmann, G., 2011. Towards quantitative sea ice reconstructions in the northern North Atlantic: a combined biomarker and numerical modelling approach. Earth Planet. Sci. Lett. 306, 137–148.
Nielsen, N., Humlum, O., Hansen, B.U., 2001. Meteorological Observations in 2000 at the Arctic Station, Qeqertarsuaq (69°15′N), Central West Greenland. Dan. J. Geogr. 101, 155–157.
Polyakova, Y.I., 2001. Late Cenozoic evolution of northern Eurasian marginal seas based on the diatom record. Polarforschung 69, 211–220.
Ramsey, C.B., 2008. Deposition models for chronological records. Quat. Sci. Rev. 27, 42–60.
Ran, L., Jiang, H., Knudsen, K.L., Eiríksson, J., 2011. Diatom-based reconstruction of palaeoceanographic changes on the North Icelandic shelf during the last millennium. Palaeogeogr. Palaeoclimatol. Palaeoecol. 302, 109–119.
Rayner, N.A., Parker, D.E., Horton, E.B., Folland, C.K., Alexander, L.V., Rowell, D.P., Kent, E.C., 2003. Global analyses of sea surface temperature, sea ice, and night marine air temperature since the late nineteenth century. J. Geophys. Res. 108, 4407.
Reimer, P.J., Baillie, M.G.L., Bard, E., Bayliss, A., Beck, J.W., Blackwell, P.G., Ramsey, C.B., Buck, C.E., Burr, G.S., EDWARDS, R.L., Friedrich, M., Grootes, P.M., Guilderson, T.P., Hajdas, I., Heaton, T.J., Hogg, A.G., Hughen, K.A., Kaiser, K.F., Kromer, B., McCormac, F.G., Manning, S.W., Reimer, R.W., Richards, D.A., Southon, J.R., Talamo, S., Turney, C.S.M., van der Plicht, J., Weyhenmeyer, C.E., 2009. IntCal09 and Marine09 radiocarbon age calibration curves, 0–50,000 years cal BP. Radiocarbon 51, 1111–1150.
Ren, J., Jiang, H., Seidenkrantz, M.-S., Kuijpers, A., 2009. A diatom-based reconstruction of Early Holocene hydrographic and climatic change in a southwest Greenland fjord. Mar. Micropaleontol. 70, 166–176.
Ribeiro, S., Moros, M., Ellegaard, M., Kuijpers, A., 2012. Climate variability in West Greenland during the past 1500 years: evidence from a high-resolution marine palynological record from Disko Bay. Boreas 41, 68–83.
Roncaglia, L., Kuijpers, A., 2004. Palynofacies analysis and organic-walled dinoflagellate cysts in late-Holocene sediments from Igaliku Fjord, South Greenland. The Holocene 14, 172–184.
Ruzmaikin, A., Feynman, J., Jiang, X., Noone, D.C., Waple, A.M., Yung, Y.L., 2004. The pattern of northern hemisphere surface air temperature during prolonged periods of low solar output. Geophys. Res. Lett. 31, L12201.
Sarnthein, M., Pflaumann, U., Weinelt, M., 2003. Past extent of sea ice in the northern North Atlantic inferred from foraminiferal paleotemperature estimates. Paleoceanography 18, 1047.
Schramm, J.L., Holland, M.M., Curry, J.A., Ebert, E.E., 1997. Modeling the thermodynamics of a sea ice thickness distribution: 1. Sensitivity to ice thickness resolution. J. Geophys. Res. 102, 23079–23091.
Seidenkrantz, M.-S., 2013. Benthic foraminifera as palaeo sea-ice indicators in the subarctic realm — examples from the Labrador Sea–Baffin Bay region. Quat. Sci. Rev. 79, 135–144.
Seidenkrantz, M.-S., Aagaard-Sørensen, S., Sulsbrück, H., Kuijpers, A., Jensen, K.G., Kunzendorf, H., 2007. Hydrography and climate of the last 4400 years in a SW Greenland fjord: implications for Labrador Sea palaeoceanography. The Holocene 17, 387–401.
Seidenkrantz, M.-S., Roncaglia, L., Fischel, A., Heilmann-Clausen, C., Kuijpers, A., Moros, M., 2008. Variable North Atlantic climate seesaw patterns documented by a late Holocene marine record from Disko Bugt, West Greenland. Mar. Micropaleontol. 68, 66–83.
Sejrup, H.P., Lehman, S.J., Haflidason, H., Noone, D., Muscheler, R., Berstad, I.M., Andrews, J.T., 2010. Response of Norwegian Sea temperature to solar forcing since 1000 A.D. J. Geophys. Res. 115, C12034.
Sha, L., Jiang, H., Knudsen, K.L., 2012. Diatom evidence of climatic change in Holsteinsborg Dyb, west of Greenland, during the last 1200 years. The Holocene 22, 347–358.
Solignac, S., Seidenkrantz, M.-S., Jessen, C., Kuijpers, A., Gunvald, A.K., Olsen, J., 2011. Late-Holocene sea-surface conditions offshore Newfoundland based on dinoflagellate cysts. The Holocene 21, 539–552.
Steinhilber, F., Abreu, J.A., Beer, J., Brunner, I., Christl, M., Fischer, H., Heikkilä, U., Kubik, P.W., Mann, M., McCracken, K.G., Miller, H., Miyahara, H., Oerter, H., Wilhelms, F., 2012. 9400 years of cosmic radiation and solar activity from ice cores and tree rings. Proc. Natl. Acad. Sci. 109, 5967–5971.
Stern, H.L., Heide-Jørgensen, M.P., 2003. Trends and variability of sea ice in Baffin Bay and Davis Strait, 1953–2001. Polar Res. 22, 11–18.
Syvertsen, E.E., Hasle, G.R., 1984. *Thalassiosira bulbosa* Syvertsen, sp. nov., an Arctic marine diatom. Polar Biol. 3, 167–172.
Tang, C.C.L., Ross, C.K., Yao, T., Petrie, B., DeTracey, B.M., Dunlap, E., 2004. The circulation, water masses and sea-ice of Baffin Bay. Prog. Oceanogr. 63, 183–228.
Tedesco, L., Vichi, M., Haapala, J., Stipa, T., 2009. An enhanced sea-ice thermodynamic model applied to the Baltic sea. Boreal Environ. Res. 14, 68–80.
ter Braak, C.J.F., 1986. Canonical correspondence analysis: a new eigenvector technique for multivariate direct gradient analysis. Ecology 67, 1167–1179.
Valeur, H.H., Hansen, C., Hansen, K.Q., Rasmussen, L., Thingvad, N., 1997. Physical environment of eastern Davis Strait and northeastern Labrador Sea. Danish Meteorological Institute Technical Report, Copenhagen.

Vare, L.L., Massé, G., Gregory, T.R., Smart, C.W., Belt, S.T., 2009. Sea ice variations in the central Canadian Arctic Archipelago during the Holocene. Quat. Sci. Rev. 28, 1354–1366.
Vinje, T., 2001. Anomalies and trends of sea-ice extent and atmospheric circulation in the Nordic Seas during the Period 1864–1998. J. Clim. 14, 255–267.
Vinnikov, K.Y., Robock, A., Stouffer, R.J., Walsh, J.E., Parkinson, C.L., Cavalieri, D.J., Mitchell, J.F.B., Garrett, D., Zakharov, V.F., 1999. Global warming and Northern Hemisphere sea ice extent. Science 286, 1934–1937.
von Quillfeldt, C.H., 1996. Ice algae and phytoplankton in north Norwegian and Arctic waters: species composition, succession and distribution. University of Tromsø pp. 1–250.
von Quillfeldt, C.H., 2000. Common diatom species in arctic spring blooms: their distribution and abundance. Bot. Mar. 43, 499–516.
Wagner, B., Melles, M., Hahne, J., Niessen, F., Hubberten, H.-W., 2000. Holocene climate history of Geographical Society Ø, East Greenland — evidence from lake sediments. Palaeogeogr. Palaeoclimatol. Palaeoecol. 160, 45–68.
Walsh, J.E., 1978. A data set on Northen Hemisphere sea ice extent, World Data Center-A for Glaciology (Snow and Ice). Glaciological Data, Report GD-2, pp. 49–51.
Weckström, K., Massé, G., Collins, L.G., Hanhijärvi, S., Bouloubassi, I., Sicre, M.-A., Seidenkrantz, M.-S., Schmidt, S., Andersen, T.J., Andersen, M.L., Hill, B., Kuijpers, A., 2013. Evaluation of the sea ice proxy IP25 against observational and diatom proxy data in the SW Labrador Sea. Quat. Sci. Rev. 79, 53–62.
Weidick, A., Bennike, O., 2007. Quaternary glaciation history and glaciology of Jakobshavn Isbræ and the Disko Bugt region, West Greenland: a review. Geol. Surv. Den. Green. Bull. 14, 1–78.
Weidick, A., Oerter, H., Reeh, N., Thomsen, H.H., Thorning, L., 1990. The recession of the Inland Ice margin during the Holocene climatic optimum in the Jakobshavn Isfjord area of West Greenland. Glob. Planet. Chang. 2, 389–399.
Weidick, A., Kelly, M., Bennike, O., 2004. Late Quaternary development of the southern sector of the Greenland Ice Sheet, with particular reference to the Qassimiut lobe. Boreas 33, 284–299.
Williams, K.M., 1986. Recent Arctic marine diatom assemblages from bottom sediments in Baffin Bay and Davis Strait. Mar. Micropaleontol. 10, 327–341.